Mitochondrial Morphology in Muscles and Neurons following Exercise and Exercise-mediated Regeneration

A Dissertation submitted

by

Aarya Mahendraa Patil

under the supervision

of

Dr. Anindya Ghosh-Roy

to the

National Brain Research Centre Gurgaon

in partial fulfillment of the requirements for the degree

of **Master of Science in Neuroscience**

June 2025

DrillBit

The Report is Generated by DrillBit Plagiarism Detection Software

Submission Information

Author Name	Aarya Mahendraa Patil
Title	Morphological Profiling of Mitochondria in Muscles and Neurons after Exercise and Exercise-mediated Regeneration
Paper/Submission ID	3928807
Submitted by	ddlal@nbrc.ac.in
Submission Date	2025-06-23 14:51:58
Total Pages, Total Words	42, 9756
Document type	Thesis

Result Information

Similarity **2 %**

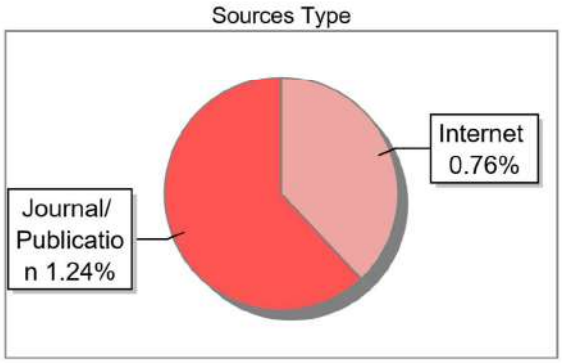

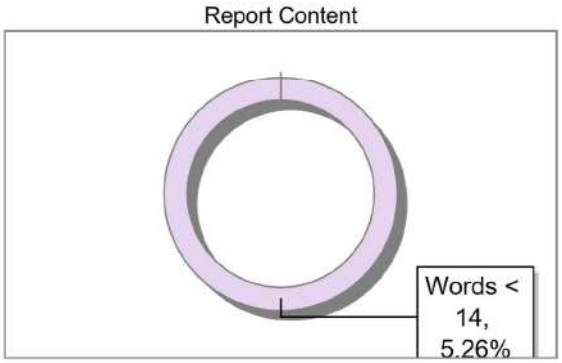

Exclude Information

Quotes	Excluded
References/Bibliography	Excluded
Source: Excluded < 14 Words	Excluded
Excluded Source	**0 %**
Excluded Phrases	Excluded

Database Selection

Language	English
Student Papers	Yes
Journals & publishers	Yes
Internet or Web	Yes
Institution Repository	Yes

A Unique QR Code use to View/Download/Share Pdf File

ब्रिक – राष्ट्रीय मस्तिष्क अनुसंधान केंद्र
BRIC – National Brain Research Centre
(जैव प्रौद्योगिकी अनुसंधान एवं नवाचार परिषद, भारत सरकार)
एन० एच०–08, मानेसर–122 052 (हरियाणा), भारत
(An Institute of the Biotechnology Research and Innovation Council, Govt. of India)
NH-08, Manesar - 122 052 (Haryana), INDIA

CERTIFICATE

is is to certify that the dissertation report entitled "**Morphological profiling of mitochondria in muscles d neurons following exercise and exercise-mediated neuronal regeneration**" is the result of work carried t by **Aarya Mahendraa Patil** in the Division of **Molecular Neurosciences**, National Brain Research Centre, nesar, India, for the fulfilment of the requirements for the M.Sc. in Neuroscience's degree.

e work presented herein is original and has not been submitted previously for the award of any degree or ploma to **National Brain Research Centre (Deemed to be University)** or to any other University. This work based on the guidelines of **National Brain Research Centre (Deemed to be University)** and is a record of candidate's own efforts.

Anindya Ghosh Roy
upervisor)

(Director, NBRC)

ace: Manesar
te: 23/6/25

दूरभाष / Telephone : +91-124-2845200 फैक्स / Fax : +91-124-2338910
ई-मेल / E-mail : info.nbrc@nbrc.ac.in Website : www.nbr

DECLARATION BY CANDIDATE

I, Aarya Mahendraa Patil, hereby declare that the work presented in the dissertation report entitled "***Morphological profiling of mitochondria in muscles and neurons following exercise and exercise-mediated regeneration***" was carried out by me under the guidance of Dr. Anindya Ghosh-Roy Division of Molecular Neuroscience at National Brain Research Centre (Deemed to be University), Manesar, Haryana, India.

I declare that no part of the thesis contains any plagiarized material. Any previously published or other material sourced from anywhere else has been appropriately attributed to the source.

I also declare that no part of this thesis has been previously submitted for the award or any degree or diploma to National Brain Research Centre (Deemed to be University) or to any other university.

Place: Manesar, Gurgoan.

Date: 23/06/2025

Aarya Mahendraa Patil.

Table of Contents

List of Figures 7
Acknowledgements 9
Graphical Abstract 10
Abstract 11
Chapter 1: Introduction 13
1.1 Mitochondria in Neurons 13
1.1.1 High Energy Demand in Neurons 13
1.1.2 Calcium Homeostasis in Neurons 14
1.2 Exercise and Mitochondria 15
1.2.1 Exercise and Muscular Mitochondria 15
1.2.2 Exercise and Neuronal Mitochondria 16
1.3 Axonal Injury and Regeneration in PNS neurons 19
1.3.1 Injury Signalling 19
1.3.2 Mitochondria-associated signalling effectors 20
1.4 Mitochondrial Dynamics 22
1.4.1 Fusion 22
1.4.2 Fission 23
1.4.3 Regulation of Fusion and Fission 23
1.4.4 Role of Mitochondrial Dynamics 23
1.4.5 Mitochondrial Transport 24
1.4.6 Mitochondrial Biogenesis 24
1.5 AMPK signalling pathway 25
1.5.1 Structure of AMPK 25
1.5.2 AMPK and Mitochondrial Dynamics 26
1.6 *C. elegans*: A Model System 26
1.6.1 The PLM Neuron for Investigating Axon Regeneration 27
Chapter 2: Rationale and Objectives 28
2.1 Exercise, muscle mitochondria and aging 28
2.2 Exercise, axotomy and neuronal regeneration 28
2.3 Rationale 29
2.4 Objectives 30
Chapter 3: Materials and Methods 31

3.1 *C. elegans* strains....31
3.2 Age-synchronisation of worms....31
3.3 Swim Exercise Assay....32
3.4 Imaging....32
3.4.1 Epifluorescence Imaging....32
3.4.2 Confocal Imaging....32
3.5 Axotomy with femtosecond laser....33
3.6 Image Processing....33
3.6.1 Muscle Mitochondrial Morphology Classification....33
3.6.2 Neuronal Mitochondrial Morphology Parameters....34
3.7 Statistics....35
Chapter 4: Results....39
4.1 Muscular Mitochondria....39
4.1.1 Wild-type Animals....39
4.1.2 *aak-2* Mutant....39
4.1.3 *mdt-15* Mutant....39
4.2 Neuronal Mitochondria in Wild-type Animals....43
4.2.1 Average Aspect Ratio....43
4.2.2 Inter-mitochondrial Distance (IMD)....43
4.2.3 Mitochondrial Load....44
4.2.4 Mitochondrial Density....44
4.2.5 Average Mitochondrial Area....44
4.3 Mitochondrial Morphology in axotomized and exercised worms....48
Chapter 5: Discussion....49
Chapter 6: Limitations and Future Directions....51
References....53

List of Figures

Figure 1: Schematic representing the regulation of neuronal regeneration after axonal injury. Adapted from Richardson et al. (2019) (18). 18

Figure 2: Mitochondrial dynamics and transport in C. elegans neurons. A) The cycle of mitochondrial fusion and fission along with their respective components. B) Anterograde and retrograde transport of mitochondria based on microtubule motors. Adapted from Onraet et al. (2024) (26). 21

Figure 3 :Mitochondrial dynamics perturbations in muscles due to exercise. The statistical significance was determined using the Chi-Square test. A) Schematic of the methodology followed. B) Representative images of the different classes of mitochondrial morphology observed. C) Bar plot showing the wild-type morphology after exercise. Animals = 24-26, n (muscle cells) = 55-62, N = 2. D) Mitochondrial morphology of aak-2 mutants after exercise. Animals = 14-18, n = 44-50, N = 1. E) Mitochondrial morphology of mdt-15 mutants after exercise. Animals = 14-15, n = 35-37, N = 1. 38

Figure 4: Mitochondrial morphology of neurons in wild-type worms after exercise. A) Schematic of the methodology followed. B) Schematic of the parameters measured for mitochondrial morphology. C) Representative images of A3 worms. D) Representative images of L4 worms. Scale bar = 10 µm 42

Figure 5: Quantification of parameters for mitochondrial morphology of L4 and A3 worms with differing recovery durations. A) Aspect Ratio, B) Intermitochondrial Distance, C) Mitochondrial Density, D) Mitochondrial Load, and E) Average Mitochondrial Area. Statistical significance was determined using two-way ANOVA with post-hoc Tukey's HSD. n = 38-52, N = 3-4. 46

Figure 6: Mitochondrial morphology in A3 worms after axotomy and exercise, with a recovery of 12 hours. A) Schematic of the methodology followed. B) Representative images of A3 worms. Scale bar = 10 µm. C) Quantification of morphology

parameters. Statistical significance was determined using Student's T test (parametric) with Bonferroni correction. n = 14-16, N = 3. 47

Acknowledgements

The first being that deserves my gratitude is the *C. elegans* nematode worm itself. Without it, neuroscience, developmental biology, and genetics wouldn't be as accomplished as they are, let alone this thesis. Working with this worm has instilled new-found awe in me towards biology and neuroscience. I have also learnt to be patient and steadfast while working with these creatures. I hope to continue my research work with this beautiful organism.

I would next like to thank Dr. Anindya Ghosh-Roy and Dr. Sibaram Behera for their contribution to this work. Dr. Ghosh-Roy always provided me with new trajectories to explore within this project. Dr. Behera has taught me everything I know about working with *C. elegans*, and I will be eternally indebted to him for this. His patience and clarity of thought are indispensable in research, which I also find very inspiring.

The lab members of the Ghosh-Roy lab have made me feel warm and welcomed throughout the duration of this project. The cheerful birthday celebrations and lab meetings will always be in my memory. Thank you for the pleasant time I got to share with you all.

I would like to thank my parents and siblings for supporting me unconditionally and lending me an ear when an experiment didn't go as planned. Thank you for always being there for me.

I also specially thank Dr. Sandhya Koushika and her lab for cordially providing me with the NBR-608 strain. This reagent formed the foundation of this project.

Graphical Abstract

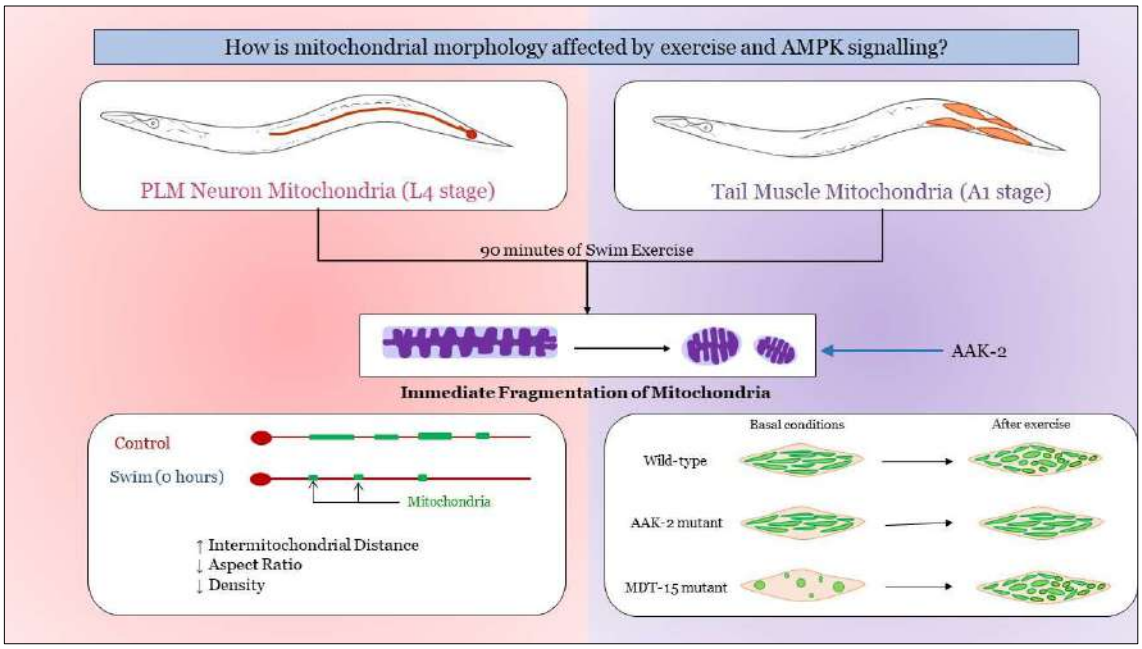

Abstract

Strategies for enhancing neuronal regeneration and functional recovery after injury have been under intense scrutiny. Exercise is known to play a role in neuronal functional restoration through AMPK signalling. Exercise also slows down aging and the decline in physical fitness though the AMPK signalling pathway. Mimicking these exercise effects by constitutively activating the AMPK signalling pathway also shows an equivalent reduction in aging-related physical fitness decline. AMPK signalling pathway in this case implements changes in mitochondrial dynamics of muscle cells, causing the cells to better adapt to exercise-induced energy requirements. AMPK is also known to physically interact with factors that control mitochondrial morphology, like Mitochondrial Fission Factor (MFF-1). Any hinderance in mitochondrial dynamics leads to the dwindling of exercise-enhanced slowing of aging, implying that AMPK signalling is acting through the mitochondrial network in the muscles to alleviate effects of aging. Similarly, it can be hypothesized whether the AMPK signalling could be functioning through the neuronal mitochondrial network to confer better functional recovery in axotomized neurons.

To further explore this hypothesis, baseline responses of the muscular and neuronal mitochondrial network to exercise are assessed in wild-type animals. Next, the morphology of mitochondria in muscles of *aak-2* and *mdt-15* mutants was determined after exercise. Both *aak-2* and *mdt-15* are involved in AMPK signalling. Lastly, the combined effect of axotomy and exercise in neuronal mitochondria was determined.

In muscles and neurons, it was observed that wild-type animals show an immediate fragmentation of the mitochondrial network. Muscle mitochondrial networks recover from this fragmentation within 12 hours. In *aak-2* mutants, there is no such immediate fragmentation seen, indicating that *aak-2* can be involved in this process of fragmentation. *aak-2* mutants also show increased elongated mitochondria after 12 hours of recovery from exercise. In *mdt-15* mutants, the mitochondrial network is very fragmented at basal conditions. Due to exercise, there are increased elongated mitochondria seen.

In neurons, along with fragmentation and a subsequent reduction in the aspect ratio of individual mitochondria, there is also a reduction in intermitochondrial distance and mitochondrial density in L4 worms. No such shift in morphology was seen in A3

worms. Lastly, in axotomized A3 worms, the pooled aspect ratio of exercised worms reduces as compared to unexercised worms.

Chapter 1: Introduction

Mitochondria are an essential organelle in all multi-cellular eukaryotic life. Along with plastids, mitochondria were hypothesized by Lynn Margulis in the 1970s to have evolved from free-living bacteria by endosymbiosis with a eukaryotic host cell. The existence of their distinct translation system and DNA was put forth by Margulis in support of her endosymbiotic theory of the origin of these organelles. With technological innovations in genome sequencing, it is now understood that mitochondria are from the bacterial phylum α-Proteobacteria. However, the nature of the eukaryotic host cell and the proto mitochondrion is still under debate (1).

Mitochondria are made of a double-layered phospholipid membrane surrounding an inner matrix. They are responsible for the generation of cellular energy by metabolising nutrients in the citric acid cycle. Along with this, they are also vital for immune defence, apoptosis, reactive oxygen species (ROS) signalling and calcium homeostasis, the last of which will be discussed later in depth. Mitochondria do not exist as lone organelles in a cell, but as tubular, dynamic networks perpetually going through the processes of fusion, fission, mitogenesis and mitophagy. The dynamicity of the mitochondrial network is crucial for the maintenance of the cell, as well as cell development, and withstanding stresses which can lead to the deterioration of the cell (2). The morphology of the mitochondrial network is thus a tightly controlled process to suit cellular demands.

1.1 Mitochondria in Neurons

Neurons are polarised, excitable cells with high energy requirements and immense complexity. Much like the neuronal cytoskeleton, neuronal mitochondrial network also show polarity in terms of their morphology in the axonal and dendritic compartments. While axonal mitochondria are small and lower in density, dendritic mitochondria are more elongated and more densely packed. The degree of dynamicity is also varied, with axonal mitochondria changing their morphology more constantly than dendritic mitochondria (2). This hints to a disparate regulation of morphology in response to compartment-specific demands.

1.1.1 High Energy Demand in Neurons

Neuronal demand for ATP is high due to multiple energy-intensive processes. Maintenance of resting membrane potential and its restoration following

depolarisation require a lot of energy, along with synaptic vesicle cycling and neurotransmitter release. The transport of key nutrients, proteins, organelles, and vesicles are also a challenge neurons face, owing to their intricate cellular architecture (3).

Neurons are known to generate ATP in an activity-dependant manner locally through the process of OXPHOS (3). This implies that the spatiotemporal distribution of the mitochondrial network is vital to meet the demands of the neuron. Indeed, it has been reported that increasing synaptic activity causes a corresponding decrease in the movement of dendritic mitochondria (4). Moreover, dendritic mitochondria are also shown to gather at the base of spines during depolarisation (5).

On the other hand, reducing stimulation causes an increase in mitochondrial length and in the number of motile mitochondria (6). Alternatively, increasing activity in the axon causes mitochondria to accumulate near the synapses, with a reduction in mitochondrial length (6). Findings are varied for the behaviour of mobile mitochondria in the axon, likely arising due to the maturity of the neuronal cells, with older cells affected more by synaptic suppression and a corresponding reduction on mobile mitochondria (2). All in all, synaptic activity affects the distribution and morphology of neuronal mitochondria.

1.1.2 Calcium Homeostasis in Neurons

Buffering of cytosolic Ca^{2+} is another major function performed by mitochondria, especially at the synapse. During an action potential, an influx of Ca^{2+} is cause by the opening of voltage-gated Ca^{2+} channels at the presynaptic terminal, inducing neurotransmitter release at the synapse. The inner matrix of mitochondria sequesters Ca^{2+} by having a suitable mitochondrial membrane potential, ultimately due to the activity of the electron transport chain (ETC). Hence, mitochondria are equipped with containing cytosolic Ca^{2+}, ultimately controlling neurotransmitter release (7).

1.1.2.1 Presynaptic Ca2+ regulation

The mitochondrial inner matrix can allow the entry of Ca^{2+} ions by the voltage-dependant anion-selective channel (VDAC) and mitochondrial Ca^{2+} uniporter (MCU) (2). While the cytosolic and mitochondrial calcium concentrations are equivalent during rest, there is a stark ~10-20-fold increase in presynaptic calcium concentration during depolarization. This sudden increase is then brought back to resting

concentration exponentially. The blocking of Ca^{2+} channels in the mitochondrial matrix have shown to increase the time needed to reset the Ca^{2+} concentration back to resting levels, leading to an uninterrupted raised concentration of Ca^{2+} (9). Thus, the ability of mitochondria to buffer Ca^{2+} at the presynaptic terminal is crucial for the regulation of neurotransmitter release.

A study by Kowaltowski (9) et al. (2019) has reported the correlation between the buffering capacity of mitochondria and their morphology. By increasing the fusion of mitochondria – leading to more elongated mitochondria, the rate and maximum capacity of Ca^{2+} storage was also increased. The opposite was observed in fragmented mitochondria. The authors hypothesize that this is due to the increased volume of the matrix in fused mitochondria as compared to fragmented ones, leading to a more stable mitochondrial membrane potential favourable for Ca^{2+} sequestration.

1.1.2.2 Postsynaptic Ca^{2+} regulation

The regulation of postsynaptic Ca^{2+} by mitochondria is less well-understood. As reported by Rangaraju et al. (2018) (3), long-term potentiation (LTP) is responsible for the fission of dendritic mitochondria, along with a rise in mitochondrial Ca^{2+} concentrations. Experimentally enhancing fission and a subsequent reduction in dendritic mitochondrial size reduced Ca^{2+} concentrations to change during stimulation, leading to lower protein synthesis. Dendritic mitochondrial size can thus affect the dendritic plasticity by the buffering capacity of the mitochondria.

1.2 Exercise and Mitochondria

Exercise is a potent non-pharmacological intervention used as a treatment for various diseases, along with slowing aging. A long-term exercise routine has been shown to increase quality of life, along with slowing the progression of neurodegenerative diseases. Physical fitness is also an indicator of healthy aging in multiple species (11).

1.2.1 Exercise and Muscular Mitochondria

Exercise is an acute cellular stressor that is known to transiently affect mitochondrial morphology in muscles. Exercise-induced gains are partly granted by the mitochondrial metabolism and network changes caused by the temporary high demand for energy. During the contraction of muscles, there is an increase in Ca^{2+} concentration in the sarcoplasm, an increase in AMP or the ADP/ATP ratio, higher ROS levels, hyperthermia, and a reduction in glycogen amounts. These drastic

changes in cellular homeostasis are dealt by the cell with multiple redundant and compensatory mechanisms (12).

The main pathways involved in this include calmodulin-dependant kinases (CaMK), mitogen-activated protein kinases (ERK1-2, MAPK), mammalian target of rapamycin (mTOR) and AMP-activated protein kinase (AMPK), the last of which is be discussed in further detail. Exercise has been shown to boost the activation of these molecules. Exercise adaptation is the consequence of short-term rises in the transcription of various proteins after each session of exercise. The recurring flares of mRNA transcripts are vital to the cellular adaptation to the exercise (12). The activity of respective mRNA transcripts in the context of muscle contractile activity is distinct, but in humans it is observed that the peak induction for metabolic and muscular genes occurs 4 to 8 hours after exercise. These levels fall back to pre-exercise ones after 24 hours post-exercise (13). To conclude, exercise is known to cause changes in mitochondrial activity temporarily, and have several beneficial effects on cellular physiology.

1.2.2 Exercise and Neuronal Mitochondria

Exercise seems to confer neuroprotective alterations that can counter brain atrophy. A momentous effect of aerobic exercise on the adult human brain is the rise in hippocampal volume. Most of this volume change has been attributed to neurogenesis-related plasticity, but in other regions of the brain like the CNS, changes in the cerebral blood volume and dendritic arborization are held culpable (14).

Steib et al. (2014) (15) have shown exercise to expedite neuronal maturation and the cause a notable increase in mitochondrial volume, along with the localisation of mitochondria in dendritic segments in stem cell-derived human neurons. Moreover, genetically inhibiting the activity of dynamin-related protein 1 (Drp1) hinders neurogenesis with or without exercise. Alternatively, increasing Drp1 activity also enhances the exercise-conferred neuronal maturation. Steib et al. conclude that exercise is capable of influencing adult hippocampal neurogenesis, and that mitochondrial adaptation is necessary for this to occur. Mitochondria can thus be used as targets for increasing hippocampal neurogenesis and plasticity in therapeutic settings.

Another study by Koo et al. (2016) (16) sought to understand the effects of exercise on neuronal cell survival in the transgenic mice model of Alzheimer's disease, along with their mitochondrial dynamics. They found that exercise reduced the levels of mitochondrial beta-amyloid protein levels, with mitochondrial fission proteins like Drp1 and Fis1. There was also a corresponding increase in mitochondrial fusion proteins like Mfn1/2 and Opa1, along with neuronal cell survival factors like mitochondrial-cytochrome C/cytosolic-cytochrome C ratio and Bcl-2/Bax ratio. Behaviourally, mice after exercise also showed improved spatial learning and cognitive function as compared to mice without exercise. The authors concluded that exercise could prevent mitochondrial dysfunction caused by amyloid-beta protein and neuronal cell death, highlighting the use of exercise in prevention of Alzheimer’s disease.

The beneficial effects of exercise in neurons even in the context of neurodegenerative diseases are mediated through mitochondrial dynamics and morphology. Hence, it is observed that the signalling pathways activated by exercise may target key players in mitochondrial dynamics and function.

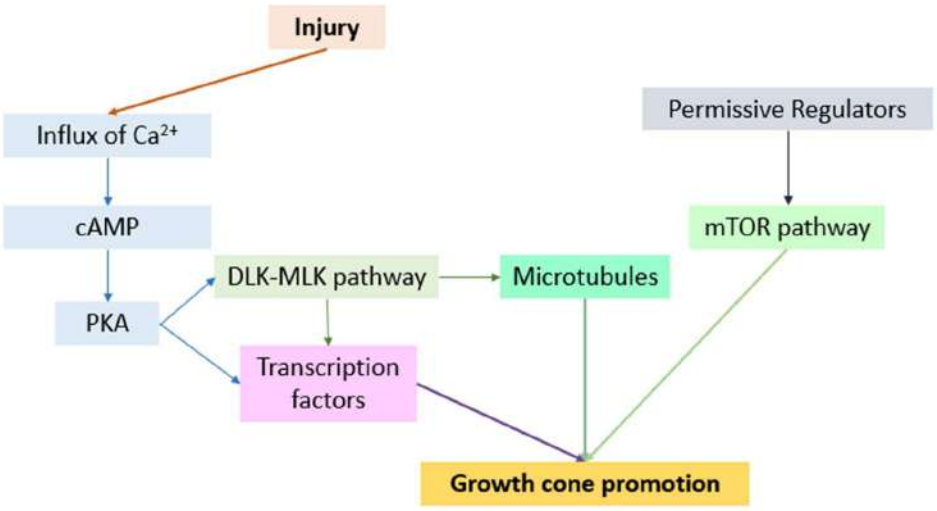

Figure 1: Schematic representing the regulation of neuronal regeneration after axonal injury. Adapted from Richardson et al. (2019) (18).

1.3 Axonal Injury and Regeneration in PNS neurons

The process of regeneration consists of a modified growth operation, in which injured axons rebuild growth cones, cytoskeleton, along with renewing synapses and former circuitry. The energy to carry out these processes originate from local mitochondria within the injured neuron (23). Injured mitochondria not only cause an energy deficiency in the cell, but also lead to the discharge of apoptotic factors (17). The mechanisms involved in CNS and PNS neuronal regeneration are very distinct, with PNS neurons showing a higher tendency to regenerate and functionally recover after injury. This work will only focus on axon regeneration of PNS neurons, which will be further discussed below.

For regeneration to occur, the injury must firstly be sensed by the neuron. It then should communicate to the nucleus to activate the repair program. There are several pathways involved in this signalling, like the DLK (dual leucine-zipper kinase-1)-MLK (mitogen-activated protein kinase) pathway, the cAMP pathway, the mTOR pathway, and so on that are summarized in the adjacent figure. The reuse of mechanisms and molecules involved in development of the neuron is seen to some degree during repair (18).

1.3.1 Injury Signalling

There are two major malfunctional molecular consequences that can initiate an injury response – calcium influx and microtubule instability. These are observed across neuronal types and species, and will be further described below.

After an injury, there is an influx of Ca^{2+} into the cytosol of the neurite that travels as a wave from the injury site to the cell body. This sharp influx activates Ca^{2+}-dependant enzymes like adenylate cyclase, which further on increases the production of cAMP. In fact, both Ca^{2+} and cAMP are shown to be necessary for axon regeneration, as genetic and pharmacological inhibition of the two have shown to deter regeneration (19).

Altered microtubule dynamics is an inevitable effect of axonal injury. Chen et al. (2015) have observed that the microtubule polymerization events near the site of injury reduce in number right after injury. In fact, axonal microtubule dynamics are inhibited by an intrinsic inhibitor of regrowth, called Exchange Factor for ARF-6 (EFA-6). The authors propose that EFA-6 is a bifunctional injury-response regulator,

playing a role at the cell cortex in maintaining microtubule dynamics in basal conditions, and at the microtubule minus ends following injury. This is yet another example of remodelling of existing signalling pathways and components for the injury response.

1.3.2 Mitochondria-associated signalling effectors

Mitochondrial signalling pathways for activating the injury response are all cell-intrinsic in nature. Some of these components can promote apoptosis under other conditions. Two important ones are discussed below.

1.3.2.1 Mitogen-activated protein kinases (MAPK)

DLK, which is a MAPK kinase kinase is a conserved regeneration-promoting signalling molecule. DLK-1 is now only activated by destabilisation of microtubules, but also by Ca^{2+} influx during injury in *C. elegans*. Crucially, in a study by Han et al. (2016), it was shown that DLK-1 promotes the relocation of mitochondria to the site of injury. This translocation was also deemed important for regeneration of the axon, as axons with a higher density of mitochondria showed greater regeneration success. The adjustment to the mitochondrial network is necessary in regenerating neurons and is mediated through DLK-1 (21).

1.3.2.2 Armadillo Repeat Containing, X Linked 1 (Armcx1)

In a study by Cartoni et al. (2016), mouse models with high regeneration capacity were used to discern the connection between mitochondrial transport and axon regeneration. Armcx1, a gene unique to placental mammals, was among many that was highly upregulated in this mice model. The authors found that Armcx1 was localised to mitochondria. Its overexpression led to better mitochondrial transport and axon regeneration. In the absence of Armcx1, regeneration capacity of the animals reduced. Moreover, it was seen that the enhanced regeneration hinged upon the localisation of Armcx1 to mitochondria. The authors thus conclude that controlling mitochondrial transport can be a therapeutic strategy to enhance axon regeneration and neuronal survival (22).

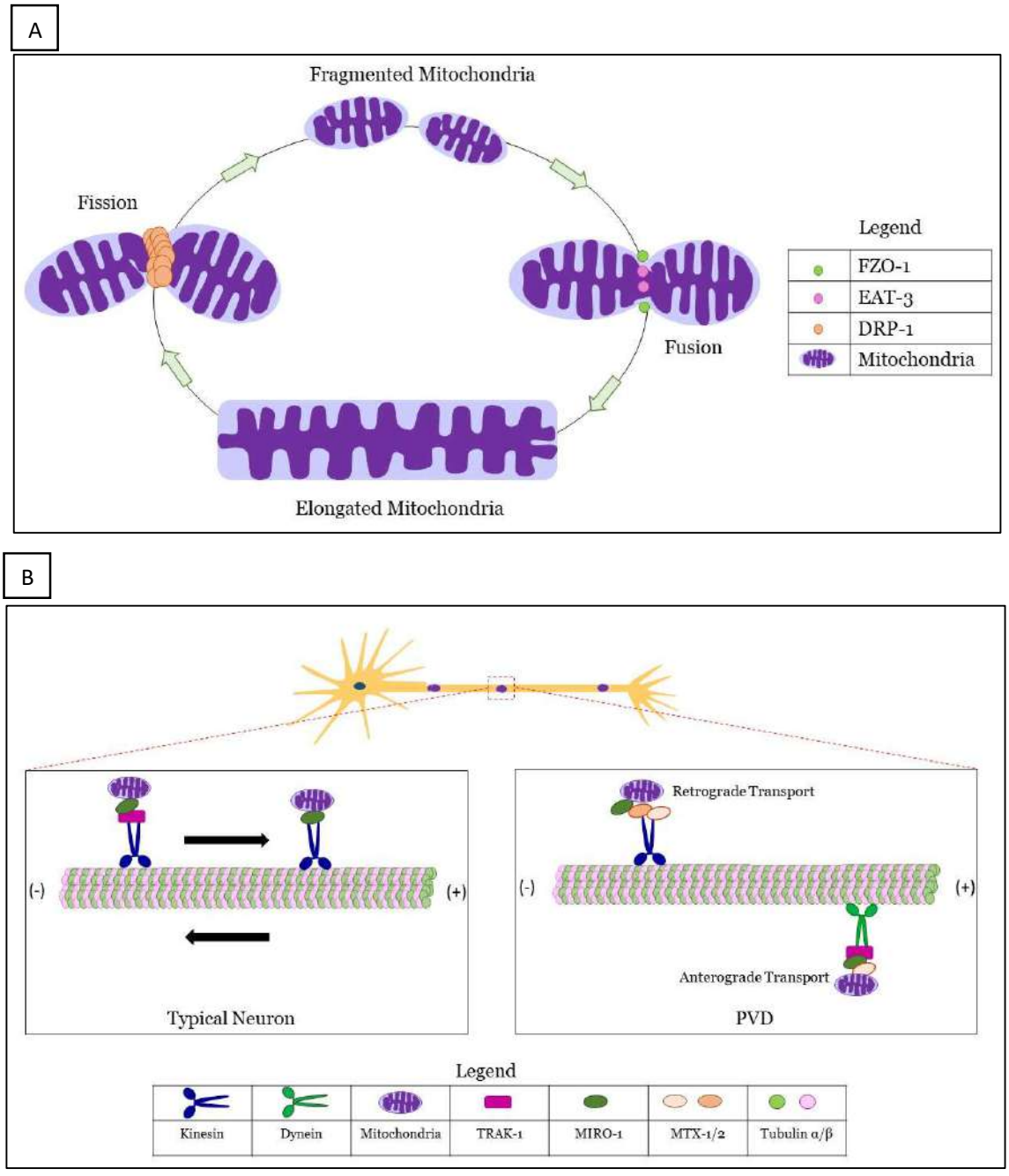

Figure 2: Mitochondrial dynamics and transport in C. elegans *neurons. A) The cycle of mitochondrial fusion and fission along with their respective components. B) Anterograde and retrograde transport of mitochondria based on microtubule motors. Adapted from Onraet et al. (2024) (26).*

1.4 Mitochondrial Dynamics

Mitochondria, as mentioned earlier, exist as highly dynamic and inter-connected organelles in the cell. Such networks can help cells tolerate and adapt to oxidative stress, mitochondrial DNA (mtDNA) mutations and nutrient deficiencies. In this section, the processes and roles performed by mitochondrial dynamics are discusses.

1.4.1 Fusion

Fusion of functional mitochondria with damaged ones can allow for the exchange of contents that can make the entire network operative. Compensation of malfunctioning components, like damaged mtDNA, and the distribution of the proteome across different cell compartments helps meet energy requirements. Fusion is accomplished by the proteins positioned on the inner and outer mitochondrial membranes (IMM and OMM). IMM and OMM fusion are disparate processes that are performed by distinct pathways, but both are aided by dynamin-related guanine triphosphatases (GTPases) (27).

In *C. elegans*, FZO-1 and EAT-3 are respectively responsible for membrane fusion of the OMM and IMM (in humans, the corresponding proteins are Mfn1/2 and Opa1). Both proteins are part of the dynamin family. FZO-1 is situated on the OMM by its transmembrane domain at the C-terminal, with its GTPase domain and hydrophobic coils project towards the cytoplasm. FZO-1 on neighbouring OMMs harness the membranes together by their hydrophobic coils. EAT-3 is similarly situated in the IMM through a mitochondrial targeting sequence (MTS) on its N-terminus. A conformational change occurs in the FZO-1 and EAT-3 after hydrolysing GTP (guanine triphosphate) to GDP (guanine diphosphate), causing the two contrasting membranes from adjacent individual mitochondria to fuse together (25, 26).

OMM and IMM fusions occur in a functionally and temporally separate fashion. OMM fusion is likely to occur upon first contact between mitochondria (27). *In C elegans*, *fzo-1* and *eat-3* mutants show not only structural aberrations in mitochondria, but are also insufficient in meeting bioenergetic and physiological needs of the organism. These mutants are shown to produce less ATP and absorb less oxygen than wild-type animals (24).

1.4.2 Fission

The process of fusion is contrasted with fission, which is the division of mitochondria. Fission is mediated in *C. elegans* by dynamin-related protein DRP-1 (in humans, Drp1), a GTPase. Like FZO-1, the activity of DRP-1 is also dependant on the hydrolysis of GTP to GDP. DRP-1 consists of a GTPase domain at the N-terminal and a GTPase effector domain (GED) at the C-terminal, which is responsible for the oligomerization with other DRP-1 molecules and GTPase activity. DRP-1 molecules homolitically bind together and form ring-like multimeric complexes that surround the surface of mitochondrion. They then confine and consecutively separate mitochondrial membranes (26, 27).

In *C. elegans*, an overexpression of drp-1 results in hyperfragmentation of mitochondria. However, these mitochondria have fused OMMs, hinting that DRP-1 mediates only OMM fission and that the two membranes go through fission independently (29). The process of IMM fission remains elusive.

1.4.3 Regulation of Fusion and Fission

At basal states, mitochondria undergo fusion and fission spontaneously. But there are several mechanisms through which these processes are orchestrated in different contexts and stimuli. Some such mechanisms are briefly discussed below.

In rat cells, Drp1 was found to be reversibly phosphorylates by c-AMP-kinase (PKA). This promoted fusion by inactivating the interaction between the GED domain and the GTPase domain (29). Contrastingly, fission can be promoted in hippocampal cells by dephosphorylating Drp1 by calcineurin, a Ca^{2+}-sensitive enzyme (30).

Exercise has been shown to cause fusion of mitochondria in C. elegans muscle cells though the action of AMP-kinase (AMPK), which senses the depletion of ATP and causes fusion of mitochondria to meet energy demands (31). This will be discussed further in later sections. A complementary mechanism that also leads to mitochondrial fusion after exercise is the DAF-16-dependant inactivation of SPG-7 and PPGN-1. These proteases in homeostatic conditions inhibit EAT-3. The authors note that DAF-16 is necessary for fusion of mitochondria induced by physical eversion (32).

1.4.4 Role of Mitochondrial Dynamics

Fusion and fission are complementary processes that primarily perform mitochondrial quality-control. While fusion allows for exchange and inter-complementation of

functional organelles with dysfunctional ones, fission helps in both mitophagy and mitogenesis. Depolarisation of the mitochondrial membrane, which is a key signal for mitophagy, occurs due to aberrations in the OXPHOS function in stressful conditions. Mitochondrial units with a low mitochondrial membrane potential can be disconnected from the network by fission, and can be further degraded though mitophagy (27, 33).

In C. elegans, PTEN-induced kinase 1 PINK-1 is stabilised on the OMM of mitochondria with low membrane potential. It then mobilizes the E3 ubiquitin ligase PDR-1 onto the OMM, ubiquitinating it. This is recognised by autophagosomes for the mitochondrion's engulfment, leading to its degradation by lysosome fusion (33).

1.4.5 Mitochondrial Transport

The distribution of mitochondrial units across cell compartments, especially in complex cells like neurons, is coordinated by several mechanisms. Anterograde mitochondrial transport, which is from the soma to distal parts of the cell along microtubules is controlled through the creation of an adaptor complex between the mitochondrion and the microtubule motor kinesin. The OMM Rho GTPase MIRO-1 can either bind to kinesin motor complex made of UNC-116 (in mammals, KIF5 kinesin family) or by first forming a complex with the motor-binding protein TRAK-1. Kinesin light chain KLC-1 and KLC-2 are also parts of this complex (26).

Retrograde transport, i.e., movement of mitochondria to the soma, is mediated by dynein. To transport mitochondria along microtubules, dynein forms a complex with MIRO-1, TRAK-1 and metaxin MTX-2. Metaxins MTX-1 and MTX-2 are also involved in anterograde transport in the PVD neuron in *C. elegans*. Kinesin and dynein thus participate in maintaining a steady mitochondrial density in *C. elegans* neurons (26).

1.4.6 Mitochondrial Biogenesis

Mitochondrial biogenesis, or the generation of new mitochondria, is controlled by peroxisome proliferator-activated receptor γ coactivator 1α (PGC-1α) in mammals. There are no worm orthologues of this factor (26). MDT-15, a subunit of the C. elegans Mediator complex, is a transcriptional coactivator that integrates several regulatory mechanisms to synchronize metabolic and hormonal regulation of fatty

acid metabolism. PGC-1 is also known to similarly collaborate with various regulatory factors, making MDT-15 in part functionally parallel to PGC-1 (34).

Another mammalian regulator of mitochondrial biogenesis is nuclear factor erythroid 2-related factor (Nrf2). The worm orthologue for this is SKN-1 which has been observed to activate biogenesis in response to mitochondrial stress. It also seems to play a role in aging (35).

1.5 AMPK signalling pathway

AMP-activated protein kinase (AMPK) is a sensor of cellular energy depletion. It is typically activated by increasing AMP levels or an increasing ADP-ATP ratio. Cellular metabolism is then adjusted to meet the energy demands of the cell. AMPK has multiple parallel pathways that affect glucose and glycogen sensing, fatty acid and cholesterol metabolism, carbohydrate metabolism, and protein synthesis (37). However, AMPK's role only in mitochondrial dynamics will be highlighted in this section. There are several non-canonical mechanisms of AMPK signalling activation that will be discussed later in this section.

1.5.1 Structure of AMPK

AMPK is expressed in all eukaryotes (with some notable exceptions like intracellular parasites). It is a heterotrimeric complex made of catalytic α-subunits and regulatory β- and γ-subunits. In mammals, there are several genes encoding 2 α-isoforms (α1/α2), two β-isoforms (β1/β2) and three γ-isoforms (γ1/γ2/γ3) (37). In C. elegans, AMPK is composed of two catalytic α subunits, aak-1, and aak-2; two β regulatory subunits, aakb-1 and aakb-2; and five γ regulatory subunits, namely, aakg-1, aakg-2, aakg-3, aakg-4, and aakg-5 (36). The allosteric effects within these subunits and their covalent modifications are what modulate the activation of AMPK (37). This work will solely focus on aak-2 subunit of AMPK, and will be further discussed later.

The foremost mechanism of covalent activation happened by the phosphorylation of a threonine residue, known as Thr172. This residue is situated in the activation loop of the α-kinase domain (α-KD). Thr172 is phosphorylated by the upstream kinase LKB-1 (liver kinase B1) in mammals, the worm orthologue of which is PAR-4. The entire mechanism happens in three steps: allosteric activation, promotion of Thr172 phosphorylation and inhibition of dephosphorylation of pThr172 (37).

1.5.2 AMPK and Mitochondrial Dynamics

AMPK plays a role in mitochondrial homeostasis. In fully functional mitochondria, the level of ATP-ADP ratio is high, which keeps the levels of AMP low as the adenylate kinase reaction (ATP + AMP ↔ 2ADP) towards the production of ADP. When mitochondrial function is encumbered, the ADP-ATP ratio rises in the intermembrane space, driving the reaction towards a higher AMP-ATP ratio than before. This activates AMPK, leading to mitochondrial dynamics alterations to revert to the homeostatic conditions (37).

A non-canonical activation of AMPK is through Ca^{2+}/calmodulin-dependant kinase kinases (CAMKKs). CAMKK2/β is known to phosphorylate AMPK at Thr172. Nelson et al. (2019) have found a feedback mechanism between intercellular levels of Ca^{2+} and AMPK. AMPK was observed to phosphorylate and inhibit stromal interaction molecule 1 (STIM1), a molecule vital for Ca^{2+} entry into the cell. The limiting of Ca^{2+} entry into the cell was noted to be beneficial in Drosophila (38).

AMPK also plays a role in mitophagy, defined as the removal of damaged mitochondria by selective autophagy (37). As discussed already, the defective mitochondria must first be fragmented by fission before undergoing mitophagy. AMPK is known to phosphorylate mitochondrial fission factor (MFF) and/or ARMC10 (39). MFF upon activation then initiates fission by recruiting DRP-1 onto the surface of the mitochondrion (40).

Furthermore, targeted mitophagy proceeds with AMPK activating ULK1, which in turn phosphorylates the E3 ubiquitin ligase Parkin. Parkin then is translocated from the cytosol to the OMM, where PINK1 activates it if the mitochondrial membrane potential is low. Parkin then polyubiquitinates OMM proteins, which serves as a signal for mitophagy to occur (41). A pool of certain subunits of AMPK are also present on the OMM in mice and humans. This implies that AMPK act as a local sensor that readily changes the mitochondrial morphology depending on the energetic requirements of the cell (42). Hence, it is seen that AMPK signalling is imperative in regulating mitochondrial dynamics, mediating both fission and mitophagy.

1.6 *C. elegans*: A Model System

C. elegans have a well-delineated genetic and biochemical mechanisms, and completely classified developmental and cellular lineages. They possess short lifespans

and life cycles, and with a transparent body, are ideal for *in vivo* imaging. They have differentiated tissues, with a nervous and gastrointestinal system, muscles, and germ tissues that allows for an organismal understanding of experimental interventions as opposed to that garnered out of cell cultures or yeast cells. The functional outputs of certain experimental interventions can also be determined through behaviours like foraging, mating, olfactory perception, locomotion, and posture analysis in *C. elegans* (26). The utility of this organism to study axon regeneration is further detailed below.

1.6.1 The PLM Neuron for Investigating Axon Regeneration

The *C. elegans* nervous system consists of 302 neurons with a largely identical morphology. Neurons can be imaged through genetically encoded fluorescent proteins. Femtosecond laser surgery has been conducted to sever axons and study the regeneration of the damaged neurites. Different neurons show variable regenerative capabilities and time, with mechanosensory neurons showing very potent regrowth (43).

The Posterior Lateral Microtubule (PLM) neurons are a pair of mechanosensory neurons extending from the lumbar ganglion to the vulval region of the animal. Each cell is made of a long anterior neurite (~ 300 μm in adults) and a short posterior neurite. The anterior axon also ventrally forms synapses with other neurites. The PLM neurons sense gentle touch in the posterior part of the animal, which causes the worm to move in the forward direction. In the event of any damage or hinderance to the PLM, this behaviour is impaired (44). The PLM neurons are part of the larger gentle touch circuitry, which is schematically represented below.

Chapter 2: Rationale and Objectives

2.1 Exercise, muscle mitochondria and aging

Exercise alters the mitochondrial morphology and metabolism in muscles. Mitochondrial fusion and fission are vital for adaptations to exercise. In a study by Campos et al. (2023), the role of muscular mitochondria in exercise was investigated in *C. elegans*. The authors show that a single 60-minute exercise session was enough for a cycle of fragmentation and fusion after 24 hours of recovery in muscle mitochondria. Daily exercise sessions caused a stall in aging-related mitochondrial fragmentation and fitness deterioration (as evaluated by body bends per second during swim exercise). fzo-1 or drp-1 mutants, which have impaired mitochondrial fusion and fission respectively, showed no such benefits induced by exercise. This highlights the powerful function mitochondrial dynamics perform in adaptation to exercise in muscles, maintenance of fitness and the delay in aging.

Moreover, the study also finds that AMPK signalling is necessary for the exercise-induced benefits to manifest. Constitutive activation of AMPK led to increased physical fitness with age but did not have any anti-aging effects. Contrastingly, aak-2 mutants that are deficient in AMPK show a decline in physical fitness with aging even with exercise. These animals also couldn't display the benefits of exercise during aging as observed in wild-type animals.

The authors lastly explored whether the exercise-induced benefits during aging might depend on the AMPK and mitochondrial dynamics acting in tandem. Animals with constitutively activated aak-2 (CA-AAK-2) displayed a better physical fitness with aging as compared to wild-type ones. In CA-AAK-2 animals, disabling mitochondrial fusion (fzo-1) or fission (drp-1) caused the improved physical fitness during aging to be nullified. The authors with these findings thus conclude that exercise-induced enhancement seen in muscles during aging is due to AMPK regulation of mitochondrial dynamics.

2.2 Exercise, axotomy and neuronal regeneration

Functional restoration following an injury in a neuron is lowered with aging in humans and *C. elegans* alike. Physical exercise used as therapeutic interventions have been shown to improve the regeneration capacity of neurons. A study by Kumar et al. (2021) sought to discern the role of swimming in enhancing functional restoration of

PLM neurons after axotomy. It was found that a 90-minute session sufficiently improved the functional restoration of the injured axon even with aging. Without injury, this exercise paradigm also improved parameters like touch response function that decline with aging.

The exercise-enhanced functional restoration was particularly linked with the initiation of axonal regeneration. In dlk-1 and mlk-1 mutants, swimming couldn't enhance functional restoration of the injured PLM axon. The thrashing frequency of these mutants were not significantly different from those of wild-type ones, ruling out any instance of a reduced swimming capability in them. This showed that exercise was improving recovery through the axon regeneration mechanism.

Specifically, the injured axons showed enhanced regrowth and post regrowth functional recovery. Self-fusion of proximal and distal ends at the site of the injury occurred more in animals subjected to exercise after injury.

Finally, it was shown that this functional restoration is heavily determined by the AMPK signalling pathway. In aak-2 mutants, there is a similar decline in the function of the PLM neuron sensitivity to gentle touch as with wild-type animals. But this decline is not impeded by exercise as seen in wild-type animals, highlighting the necessity of aak-2 in regeneration. Moreover, both muscle- and neuronal-specific RNAi rescue of aak-2 in aak-2 mutants could revert this phenomenon, with neurons showing some functional restoration. Pharmacologically activating AMPK though metformin in paralyzed worms that could not swim was enough to simulate the functional restoration seen in those that could. In aak-2 mutants, this activation yielded no functional restoration, further bolstering the role of AMPK signalling in this phenomenon. The authors thus conclude that AAK-2 can improve functional restoration of the PLM neuron in a cell-autonomous and non-autonomous (through muscles) manner (46).

2.3 Rationale

From the studies conducted by Campos et al. (2023) and Kumar at al. (2021), it is observed that AMPK signalling is implicated in remodelling muscle mitochondrial morphology to alleviate age-related decline in fitness and in the functional restoration of neurons after axotomy. Exercise can confer improvements in both physical fitness and neuronal functional restoration through the AMPK signalling, with the former

specifically working through the adjustments in mitochondrial dynamics like fusion and fission.

However, it is still unclear whether mitochondrial dynamics are responsible for the heightened functional restoration following axotomy in exercised animals. There is plenty of evidence (47, 48), as was discussed earlier, to accentuate the role of mitochondrial dynamics and transport in neuronal regeneration. But there is still no coherent connection between exercise-enhanced functional restoration in neurons and their mitochondrial dynamics. Moreover, if there is such a connection seen, then whether AMPK signalling is behind the reorganization of mitochondria is still an unexplored aspect.

Therefore, this study pursued the exploration of these outstanding questions. To reiterate, we wanted to investigate whether mitochondria are playing a role in exercise-mediated enhancement in functional restoration of neurons after axotomy. If mitochondria are indeed influencing this, then is the AMPK signalling behind the modifications seen in their morphology. The explicit objectives of the study in investigating this are listed below.

2.4 Objectives

1. Establish a baseline for muscular mitochondrial profile in A1 wild-type animals.
2. Morphological profiling of muscular mitochondria in aak-2 and mdt-15 mutants.
3. Establish a baseline for neuronal mitochondrial profile in wild-type animals at the L4 and A3 stage.
4. Morphological profiling of mitochondria in injured axons with and without swim exercise in wild-type animals at the A3 life-stage.

Chapter 3: Materials and Methods

3.1 *C. elegans* strains

All strains were grown and maintained at 20 °C in nematode growth media (NGM). The strains used were: Bristol N2, RB754 aak-2(ok524) X, SJ4103 zcIs14 [Pmyo-3::mito::GFP], NBR-608 tbIS222; JsIs609[Pmec-7::mCherry]; [Pmec-4::MLS::gfp], XA7702 mdt-15(tm2182) III and muIs32. Transgenes for the mitochondrial marker were introduced into the aak-2(ok524) and mdt-15(tm2182) by crossing. The strains obtained were NBR1145 zcIs14(Pmyo-3::mito-GFP); aak-2(ok524) and NBR1146 zcIs14(Pmyo-3::mito-GFP); mdt-15(tm2182) was conducted to verify homozygosity for mutations.

Strain Number	**Genotype**
N2	Wildtype
RB754	aak-2(ok524) X
SJ4103	SJ4103 zcIs14 [Pmyo-3::mito::GFP]
NBR-608	tbIS222; JsIs609[Pmec-7::mCherry]; [Pmec-4::MLS::gfp]
XA7702	mdt-15(tm2182) III
NBR1145	zcIs14(Pmyo-3::mito-GFP); aak-2(ok524)
NBR1146	zcIs14(Pmyo-3::mito-GFP); mdt-15(tm2182)

3.2 Age-synchronisation of worms

NGM plates were seeded with OP50 bacteria. 40-50 gravid adults were transferred to each of these plates and maintained at 20 °C for 2 hours for egg-laying. Adult worms were then removed from the plates after this duration. Two days after the eggs were allowed to hatch, 40-50 mid-L4 worms were moved to new OP50-seeded NGM plates. They were transferred to new plates every 24 hours to get animals at the desired life stage (24 hours for A1 stage and 72 hours for A3 stage).

3.3 Swim Exercise Assay

Swim exercise as described by Laranjerio et al. (2017) (45) was adopted by this study. 200 µL of 1X M9 was added to added to each well of a 96-well plate. One worm at the desired life stage was transferred to each filled well and left undisturbed for 90 minutes. The exercised worms were recovered in seeded NGM plated with the aid of a mouth pipette. This formed the experimental cohort of the assay. For the control group, worms were transferred to an unseeded NGM plate for the same duration and then transferred to a seeded NGM plate.

For worms with 12- and 24-hour recovery after swimming, they were left in seeded NGM plates following the swimming assay. They were then imaged at the desired time point.

3.4 Imaging

3.4.1 Epifluorescence Imaging

For the assessment of neuronal mitochondrial morphology at the L4 stage, epifluorescence imaging was conducted. Worms were immobilised on 3% agarose pads made on glass slides using 10 mM levamisole hydrochloride. GFP-labelled mitochondrial in the PLM neuron at the L4 stage were imaged with the ECLIPSE Ti2 inverted microscope equipped with the Andor (iXon DU897-UVB) monochrome camera. 100X oil immersion objective with 1.45 NA was used at 1-2 µm slice interval with the 480 nm laser at an exposure time of 250 ms. The .tif images were processed and analysed in FIJI as described below.

For the assessment of muscular mitochondria in aak-2 and madt-15 mutants, the worms were similarly prepared on glass slides. Zeiss-apotome 3 upright microscope with Apotome Plus camera was used to image these worms. The 63X oil immersion objective with an NA of 1.4 was used. An exposure of 35-40 ms was provided. The muscles were imaged at 0.25 µm slice intervals. The .czi files were further processed in FIJI.

3.4.2 Confocal Imaging

For imaging neuronal mitochondria at the A3 stage, confocal microscopy was done. Worms were prepared on slides as mentioned earlier. The GFP-labelled mitochondria were imaged with either the A1 HD25/A1R HD25 microscope or the AX/AX R microscope with 60X oil immersion aperture (1.4 NA). The mitochondria were

imaged with the 488 nm laser at 2% transmission and the PLM neuron were imaged with the 560 nm laser at 5% transmission. The 25 mm FOV Galvano scanner was used for this. The images obtained were of 512 × 512-pixel resolution, a slice interval of 0.5 µm and a zoom of 1. The dwell time was 0.2 microseconds.

For the imaging of wild-type muscular mitochondria, worms were prepared as already mentioned. The AX/AX R microscope was used with the same imaging conditions. The GFP-labelled mitochondria were imaged with the 488 nm laser at 0.2% transmission, with a slice interval of 0.25 µm and a resolution of 1024 × 1024 pixels.

3.5 Axotomy with femtosecond laser

For the axotomy of PLM neurons, worms were immobilised in 0.1 µm of polystyrene beads on 3% agarose pad with a coverslip. The only one PLM neuron was axotomized with 2 pulses of the 920 nm femtosecond laser 50-60 µm away from the cell body, as described by Basu et al. (2017) (49). The worms were imaged with a 100X oil immersion objective of 1.45 NA (of the ECLIPSE Ti2 microscope) at 480 nm. Following axotomy, the worms were revived using 1X M9 and a mouth pipette onto a seeded NGM plate. They were given a recovery time of 3 hours before the 90-minute swim session, after which the PLM mitochondria imaged (with a second recovery time of 0, 12 and 24 hours) as already discussed.

3.6 Image Processing

All images were processed using FIJI. The images were first z-projected with maximum intensity to obtain a 2D image.

3.6.1 Muscle Mitochondrial Morphology Classification

C. elegans body wall muscles are arranged along the dorso-ventral axis, making their quantitative classification difficult. Hence, a qualitative classification as described by Laranjeiro at al. (2019) (50) was adopted in which mitochondrial morphology was divided into 5 classes. The descriptions of all classes are briefly listed below:

> Class 1: Tubular, elongated and well-connected mitochondrial units that completely cover the muscle cell.
>
> Class 2: Swollen, oval mitochondrial units that are somewhat fragmented with complete muscle cell coverage.

Class 3: Round, fragmented mitochondrial units with complete muscle cell coverage.

Class 4: Round, fragmented mitochondrial units with partial muscle cell coverage.

Class 5: Drastically reduced number of mitochondria with round and fragmented morphology.

The muscles from the tail to the area posterior to the vulva were chosen for this assessment as they showed consistent morphology and experienced the least distortion from eggs inside the worm. Two to four muscle cells were scored for each worm to account for the morphological variability within each animal. All scoring was conducted by the same observer under blinded conditions in which the identities of the animals were obscured.

3.6.2 Neuronal Mitochondrial Morphology Parameters

The mitochondria of the PLM neuron were quantitatively assessed. The parameters and their procurement were adopted from Mondal et al. (2021) (51) and Morsci et al. (2016) (52). The list of parameters is given below:

1) Aspect Ratio: The ratio of major axis to the minor axis of a fitted ellipse to the mitochondrial particle. This parameter is a measure of the shape of the mitochondrion, the lowest value of 1 corresponding to a perfect circular shape while any value higher than 1 indicating an elongated shape.
2) Intermitochondrial Distance (IMD): The lowest distance between the centroids of two consecutive mitochondria particles. The formula used for this is:

$$IMD = \sqrt{[(X_{n+1} - X_n)^2 + Y_{n+1} - Y_n)]}$$

3) Mitochondrial Density: The number of mitochondria per 100 µm of the axon.
4) Mitochondrial Load: Total mitochondrial area per 100 µm of the axon.
5) Mitochondria Area: The area enclosed by each mitochondria particle.

To obtain these parameters, the z-projected image was first converted to 8-bit type and background subtracted (rolling ball 30). The images were then thresholded at the Otsu setting. The particles were then analysed for the area, perimeter, major axis, minor

axis, and X-Y coordinated of the centroid. Particles with an area >0.15 μm^2 were selected and analysed further.

3.7 Statistics

All statistical tests were performed in R Studio version 4.5.0. Three or more samples with quantitative data were compared with ANOVA (parametric) with a *post hoc* Tukey's HSD. Two samples with qualitative data were compared with the Chi-square test. Two sample comparisons with quantitative data were conducted using Student's T test (parametric). Values for all are presented as *mean*.

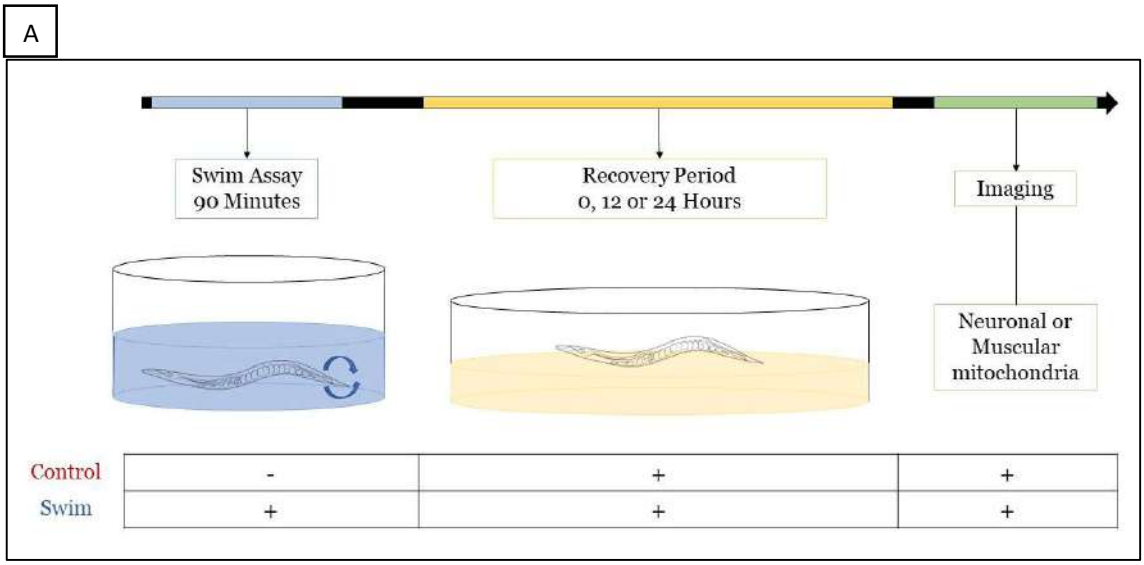

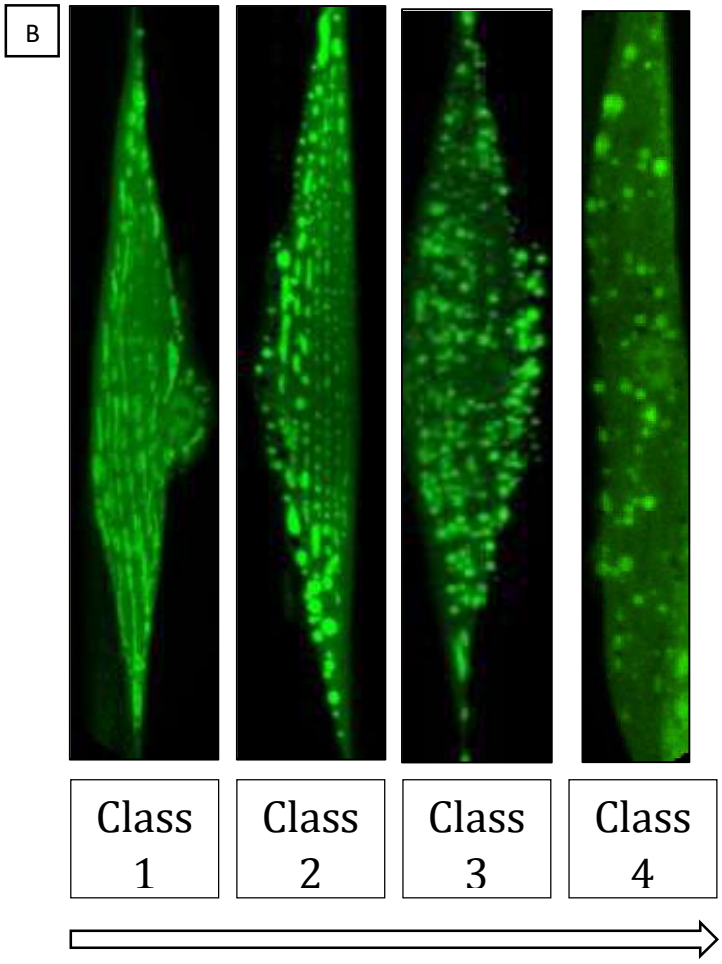

(Caption provided on the following page)

C

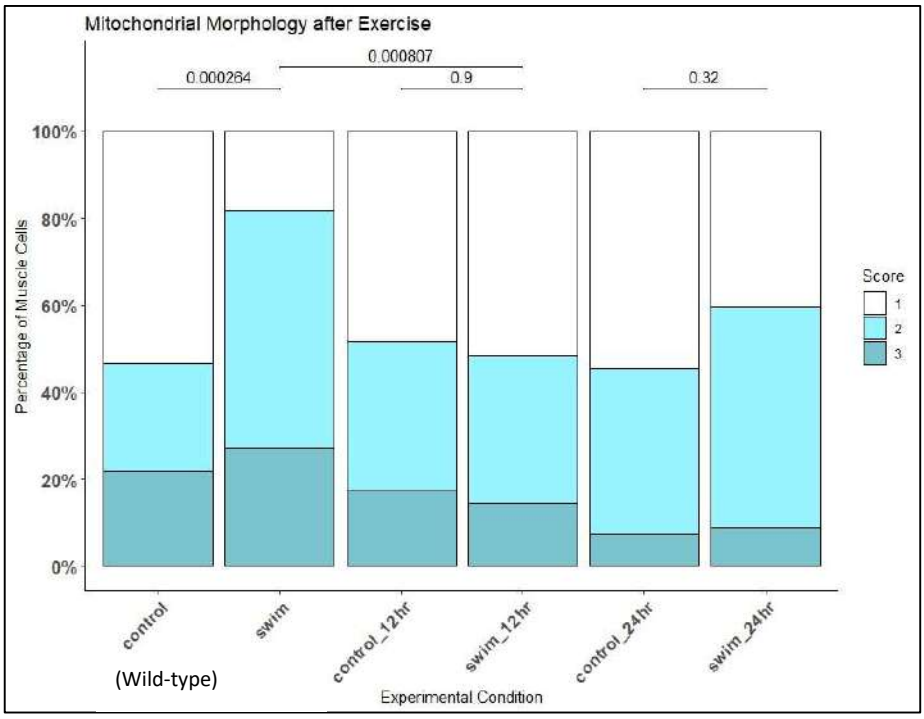

(Wild-type)

D

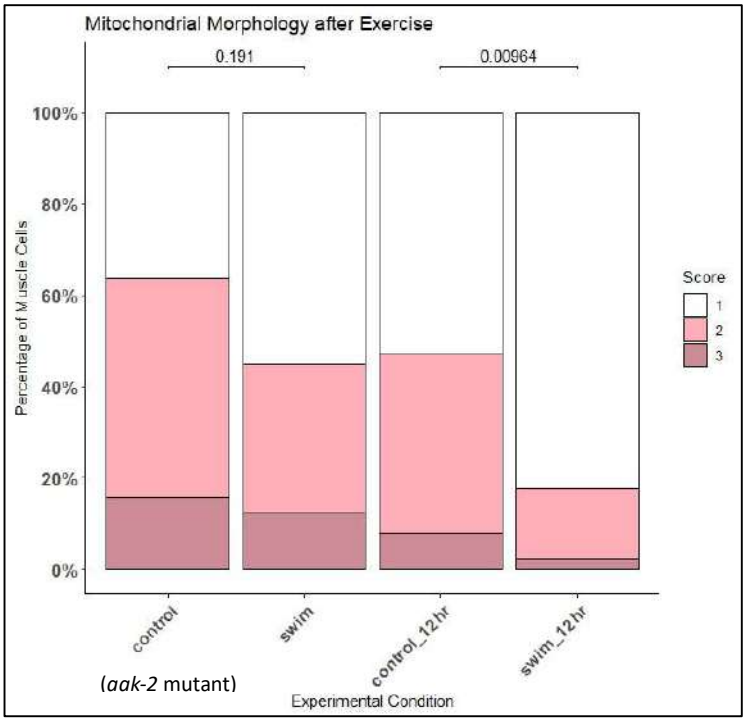

(*aak-2* mutant)

(Caption provided on the following page)

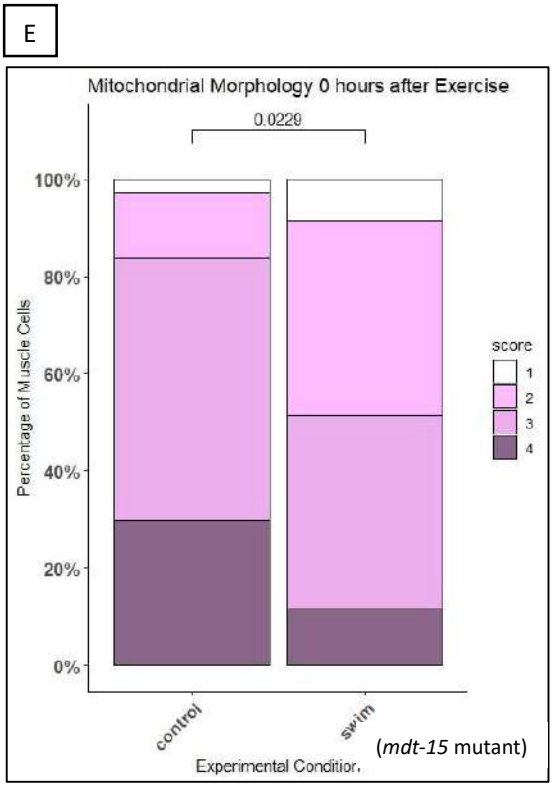

Figure 3 :Mitochondrial dynamics perturbations in muscles due to exercise. The statistical significance was determined using the Chi-Square test. A) Schematic of the methodology followed. B) Representative images of the different classes of mitochondrial morphology observed. C) Bar plot showing the wild-type morphology after exercise. Animals = 24-26, n (muscle cells) = 55-62, N = 2. D) Mitochondrial morphology of aak-2 *mutants after exercise. Animals = 14-18, n = 44-50, N = 1. E) Mitochondrial morphology of* mdt-15 *mutants after exercise. Animals = 14-15, n = 35-37, N = 1.*

Chapter 4: Results

4.1 Muscular Mitochondria

4.1.1 Wild-type Animals

To ensure that the exercise assay adopted in this study was sufficiently engaging the body wall muscles, mitochondrial morphology in wild-type animals was assessed after undergoing exercise for 90 minutes. The control animals, which were allowed to crawl on unseeded NGM plates for 90 minutes, had muscles cells with 53.3% of class 1, 25% of class 2 and 21.6% of class 3 mitochondrial morphology. In contrast, the exercised animals imaged immediately after had 18.2% of class 1, 54.5% of Class 2 and 27.3% of Class 3 muscles cells. This statistically significant rise ($p < 0.001$) of muscle cells with class 2 and 3 mitochondrial morphology and a fall in class 1 mitochondrial morphology indicates that there is a fragmentation of mitochondria in the cells due to exercise.

With a 12-hour recovery period, the mitochondrial morphology in exercised animals is identical to animals that haven't undergone exercise. The same is seen in animals provided with a 24-hour recovery period after exercise. This shows that there is an intermittent fragmentation of mitochondria in muscle cells after exercise in wild-type animals, but there is a recovery in this network disorganisation within 12 hours. This can thus serve as a baseline trend for comparison with mutant animals that are described next.

4.1.2 *aak-2* Mutant

In *aak-2(ok524)* background, muscles show no change in morphology after exercise. However, with a 12-hour recovery period, the percentage of Class 1 muscle cells dramatically increases significantly ($p < 0.05$) to 82% in exercised worms as compared to unexercised worms, which have 53% of Class 1 muscles cells. However, it is to be noted that the number of samples for this data is limited and needs further validation.

4.1.3 *mdt-15* Mutant

In the *mdt-15(tm2182)* background, muscles show an immediate change in mitochondrial morphology due to exercise. There is an increased percentage of muscles showing Class 4 mitochondrial networks at basal levels as compared to wild-type worms, which is likely due to the hindrance caused to the mitogenesis processes

in the absence of MDT-15. This makes the quality-control of mitochondrial units difficult, resulting in swollen and fragmented mitochondria.

Without any exercise, muscles show 3% of Class 1, 13% of Class 2, 54% of Class 3 and 20% of Class 4 muscle cells. Right after exercise, there is a significant increase ($p < 0.05$) in the fraction of Class 1 and Class 2 muscle cells (9% and 40% respectively), with a subsequent decrease in Class 3 and Class 4 cells (40% and 11% respectively). This shows that the mitochondrial network in the muscles of the mdt-15 mutant show increased fusion due to acute exercise, as opposed to wild-type muscles that show fragmentation of mitochondria. This differential response to swim exercise needs further validation due to the limited sample size of the data presented.

A

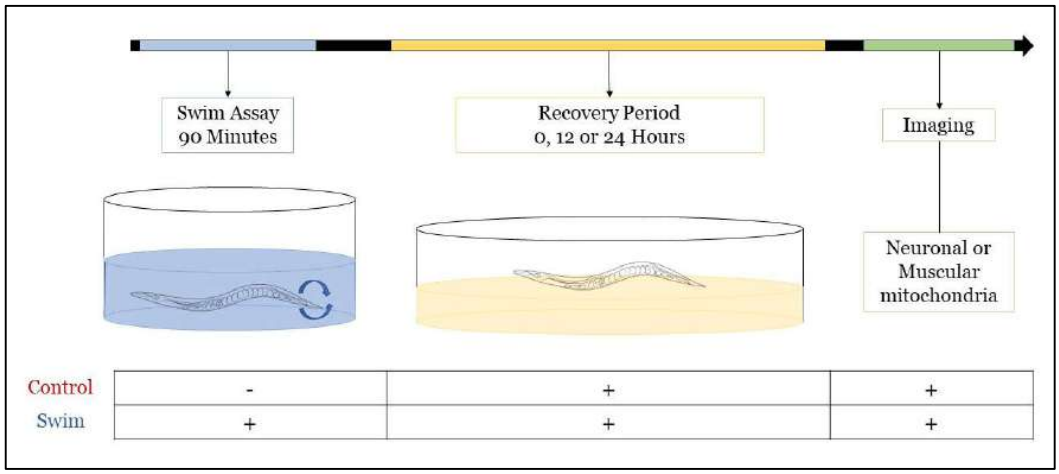
Swim Assay
90 Minutes
Recovery Period
0, 12 or 24 Hours
Imaging
Neuronal or
Muscular
mitochondria
Control
Swim
-
+
+
+
+
+

B

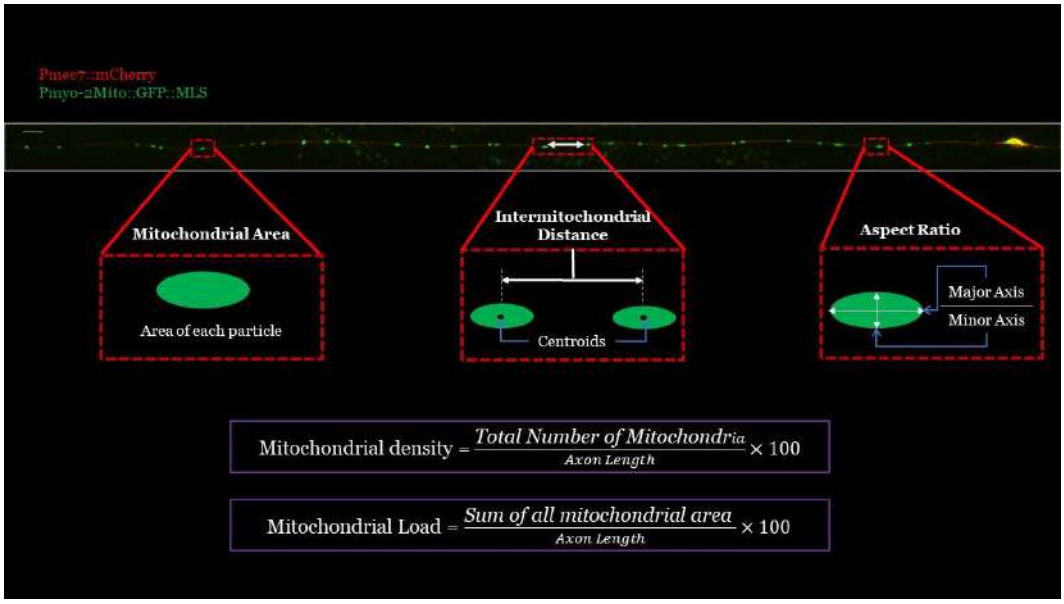
Punc67::mCherry
Pmyo-2Mito::GFP::MLS
Mitochondrial Area
Area of each particle
Intermitochondrial
Distance
Centroids
Aspect Ratio
Major Axis
Minor Axis
Mitochondrial density = Total Number of Mitochondria / Axon Length × 100
Mitochondrial Load = Sum of all mitochondrial area / Axon Length × 100

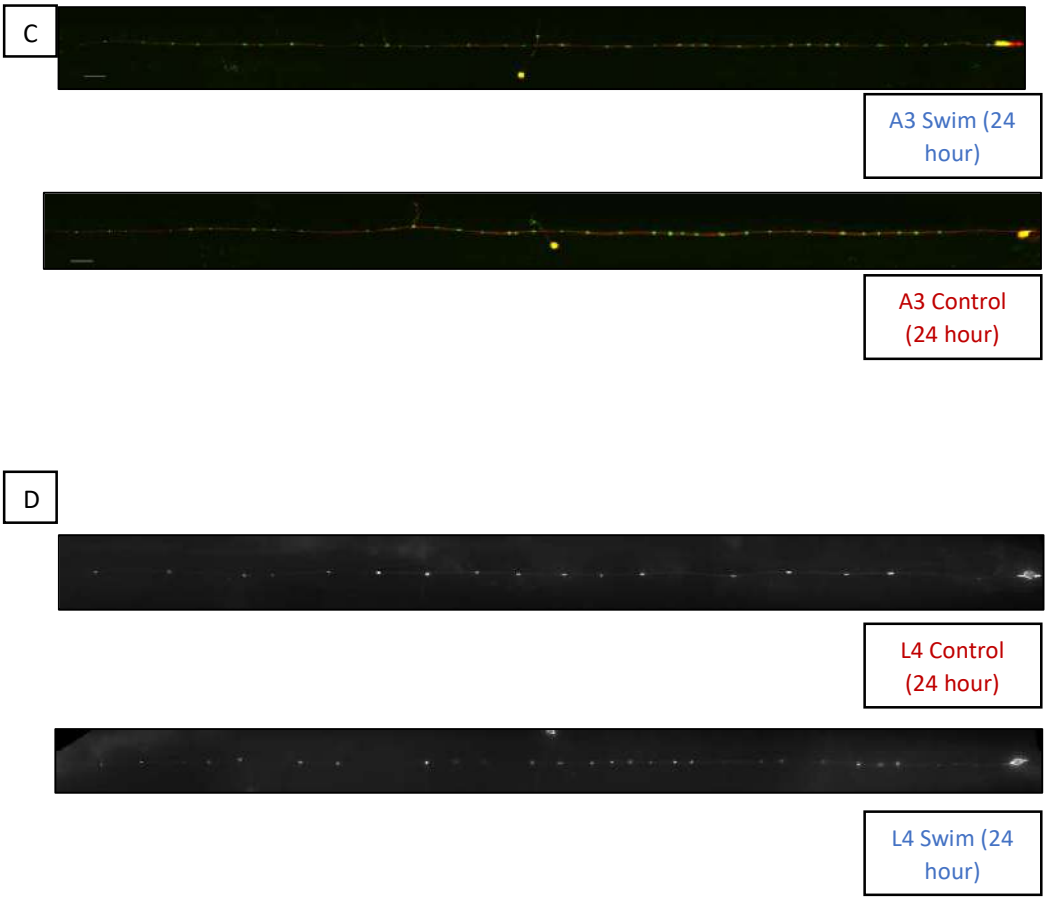

Figure 4: Mitochondrial morphology of neurons in wild-type worms after exercise. A) Schematic of the methodology followed. B) Schematic of the parameters measured for mitochondrial morphology. C) Representative images of A3 worms. D) Representative images of L4 worms. Scale bar = 10 µm

4.2 Neuronal Mitochondria in Wild-type Animals

To establish a baseline dynamic of mitochondrial morphology altered by swim exercise, neuronal mitochondria in the PLM neuron were analysed. Animals belonging to two life stages were chosen: L4, which is a transition from larval to the adult stage and corresponds to any developmental influence the mitochondrial network may have, and A3, which is an older adult stage. Kumar et al. (2021) have reported that there is a sharp decline in the functional restoration of neurons after axotomy in the A3 to A4 stage transition. This decline is deferred by the swim exercise intervention, and is thus the mitochondrial dynamics behind this are worth investigating. The time at which the mitochondrial morphology was evaluated was 0, 12 and 24 hours after exercise. L4 and A3 worms were imaged using fluorescence and confocal microscopy respectively, and thus the values measured for these are not comparable to each other.

4.2.1 Average Aspect Ratio

Aspect ratio is a measure of the shape of the mitochondria in the PLM neuron. This parameter was individually measured for each mitochondrion in the PLM neuron and an average value per neuron was then plotted. In L4 worms, the average aspect ratio significantly reduces ($p < 0.05$) from a mean of 2.42 in unexercised worms to a mean of 1.98 in exercised worms immediately after the exercise. The mitochondria then recover their original average aspect with a recovery period of 12 hours. The animals show a rise in average aspect ratio with a mean of 2.56 without any swim exercise, likely due to their growth from larva into an adult.

However, in corresponding exercised worms, there is a significant rise ($p < 0.05$) in average aspect ratio to a mean of 2.95. It can thus be seen that there is an immediate fall in aspect ratio of mitochondria due to exercise, which is then recovers after twelve hours, followed by a rise in the aspect ratio with a recovery period of 24 hours. Contrastingly, in A3 animals, there are no changes in aspect ratio due to exercise, with both control and swim groups showing non-significant variability.

4.2.2 Inter-mitochondrial Distance (IMD)

IMD is the distance of between the centroids of two consecutive mitochondria particles. It is a method of evaluating the mobility of mitochondria in the neuron. The IMD in unexercised worms is 20.85 μm at the L4 stage, while exercised worms with

no recovery period have an IMD of 24.86 μm, which significantly larger ($p < 0.005$). The are no other significant changes in either control and swim groups with recovery periods of 12 and 24 hours. The same is observed in A3 worms, with groups showing consistent IMD regardless of the recovery periods provided.

4.2.3 Mitochondrial Load

Mitochondrial load in unexercised worms at the L4 stage show a rise from 3.81 $\mu m^2/\mu m$ at 0 h to 6.09 $\mu m^2/\mu m$ at 12 h ($p < 0.005$), following a drop to 4.16 $\mu m^2/\mu m$ at 24 hours. The exercised worms don't show a significant difference in mitochondrial load at the 0 h and 24 h timepoints (3.28 $\mu m^2/\mu m$ and 4.69 $\mu m^2/\mu m$ respectively) as compared to the unexercised animals. However, at 12 h, the load of the exercised group is significantly larger ($p < 0.005$) than unexercised worms, at a value of 7.73 $\mu m^2/\mu m$. In A3 worms, there are no significant changes in mitochondrial load in exercise and unexercised worms.

4.2.4 Mitochondrial Density

In L4 worms, there is an immediate decrease in mitochondrial density right after exercise. In exercised animals, the mitochondrial density (4.25 units/μm) is significantly lower ($p < 0.05$) than the density in unexercised animals (5.07 units/μm). The density at all other timepoints due to exercise remains unchanged. The mitochondrial density remains also is non-significantly different throughout the L4 to A1 transition of unexercised worms. In A3 worms, there are no significant changed in density due to exercise at different timepoints.

4.2.5 Average Mitochondrial Area

Area enclosed by each mitochondria particle per neuron is individually measured, and an average per PLM neuron is plotted. Average mitochondrial area follows the same trend as the mitochondrial load, with L4 unexercised worms showing an intermittent significant increase ($p < 0.005$) in area at 12 h with a value of 1.07 μm^2 (as compared to 0.73 μm^2 and 0.77 μm^2 at 0 h and 24 h respectively). Due to exercise, there is an even high area increase that is significant ($p < 0.0005$) with a value of 1.35 μm^2. In A3 worms, there are no changes in average area at any timepoint even in the exercise condition.

A

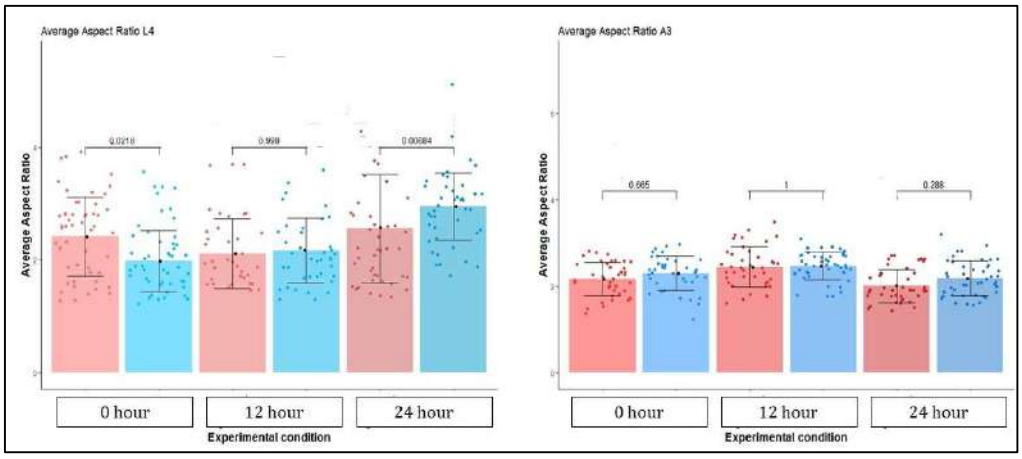

B

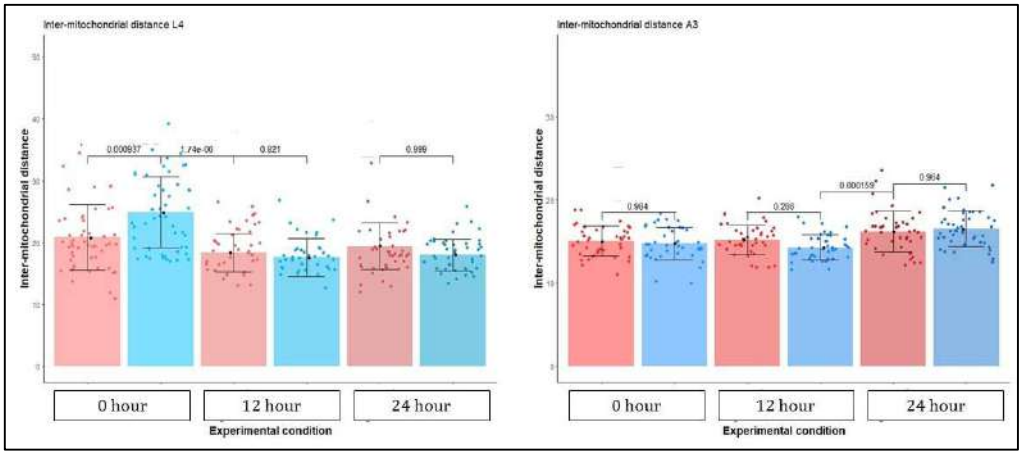

C

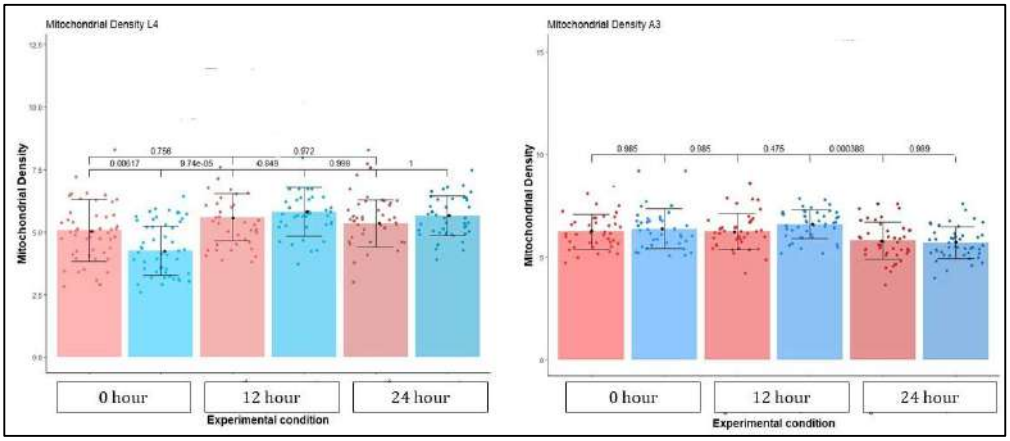

(Caption provided on the following page)

D

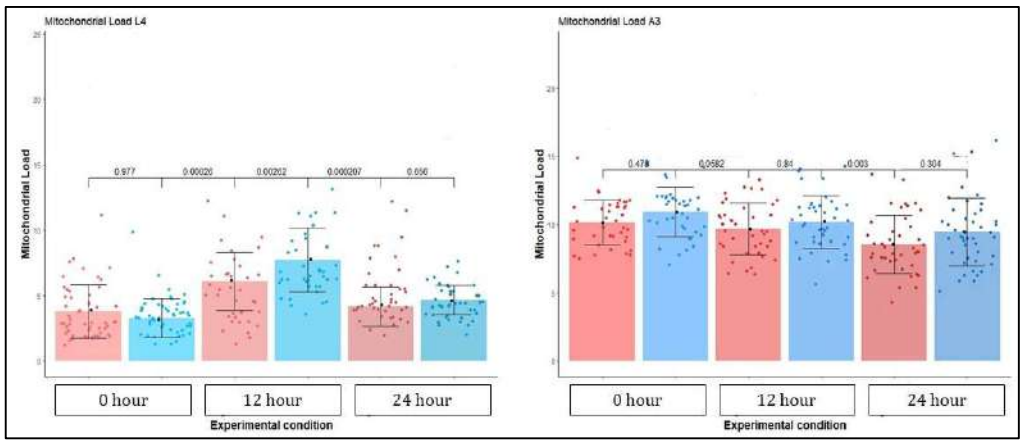

E

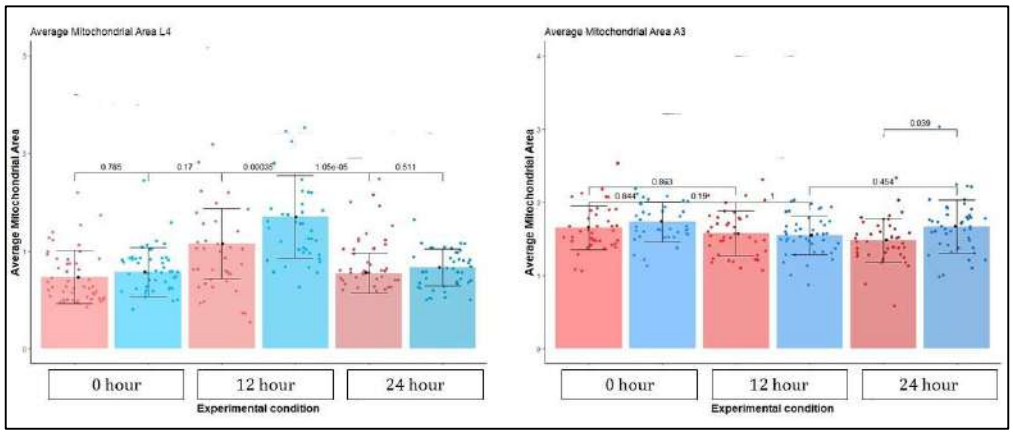

Figure 5: Quantification of parameters for mitochondrial morphology of L4 and A3 worms with differing recovery durations. All control data is represented by red bars and all exercised data is represented by blue bars. A) Aspect Ratio, B) Intermitochondrial Distance, C) Mitochondrial Density, D) Mitochondrial Load, and E) Average Mitochondrial Area. Statistical significance was determined using two-way ANOVA with post-hoc *Tukey's HSD. n = 38-52, N = 3-4.*

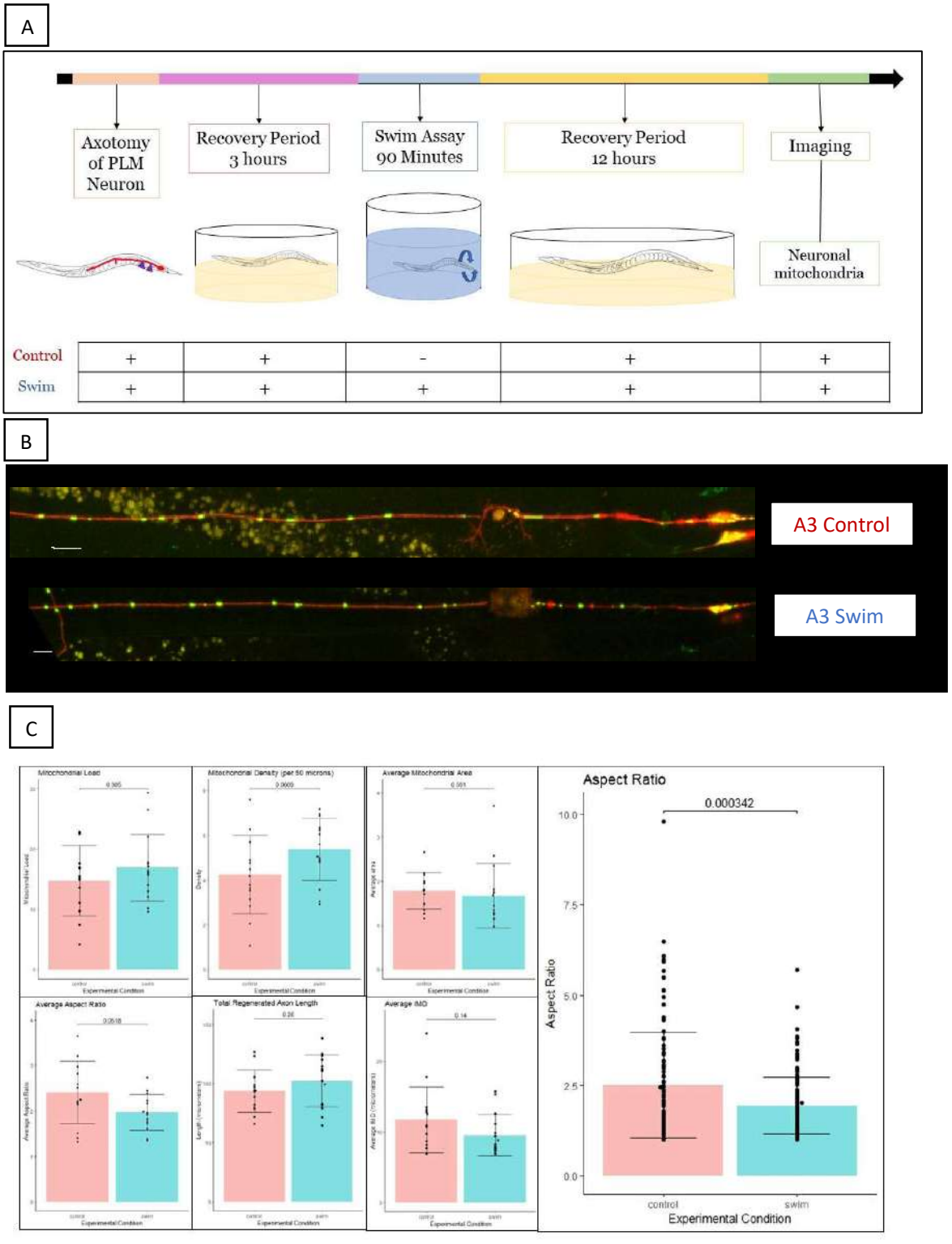

Figure 6: Mitochondrial morphology in A3 worms after axotomy and exercise, with a recovery of 12 hours. A) Schematic of the methodology followed. B) Representative images of A3 worms. Scale bar = 10 µm. C) Quantification of morphology parameters. Statistical significance was determined using Student's T test (parametric) with Bonferroni correction. n = 14-16, N = 3. All control data is represented by red bars and all exercised data is represented by blue bars.

4.3 Mitochondrial Morphology in axotomized and exercised worms

The parameters as described above were similarly measured for axotomized PLM neurons after exercise assay with a recovery period of 12 hours. The mitochondria particles present in the axon section at the site of injury proximal to the cell body taken into consideration, as the distal part of the axon undergoes degeneration if there is no fusion event. This was only done in A3 worms because of the higher survivability of A3 worms after axotomy as compared to L4 worms, and to also rule out developmental confounding factors that may cause the effects of swimming on mitochondrial morphology difficult to investigate. All worms were given 3 hours of recovery time after axotomy, following which they were either subjected to the swim exercise assay or left on unseeded NGM plates as a form of control.

The exercised worms show no significant changes in any of the parameters as listed above. The average aspect ratio of unexercised worms is borderline significantly ($p = 0.052$) higher with a value of 2.41 than that of exercised worms, with a value of 1.97. When the aspect ratio values of individual mitochondria are pooled together, the unexercised worms show a significantly higher ($p < 0.0005$) aspect ratio of 2.51 than the aspect ratio of exercised worms with a value of 1.95.

The mitochondrial density of the worms was measured as the number of mitochondrial units per 50 μm of axonal length, as only the proximal section of the axon was investigated. The exercised worms show a density of 5.38 units/μm, which is borderline significantly ($p = 0.067$) larger than the density in unexercised worms, with a value of 4.26 units/μm.

Chapter 5: Discussion

The motivation of this study was to uncover whether the exercise-enhanced functional restoration of injured axons was happening through the reorganization of mitochondrial dynamics, and if the changes in mitochondrial morphology was tied to AMPK signalling. The assessment of mitochondrial morphology in muscles as affected by exercise was conducted to ensure that there is a change in the morphology as reported (31) caused by the 90-minute swim assay. A1 worms show a fragmentation of mitochondria (estimated qualitatively) right after exercise, as already stated (31), with a recovery within 12 hours.

Furthermore, the mitochondrial morphology of *aak-2* and *mdt-15* mutants were investigated in muscles to further determine the role of AMPK signalling in determining mitochondrial dynamics. *aak-2* mutants show no immediate fragmentation after exercise, but with a 12-hour recovery time, show exercised worms show an increase in the fusion of mitochondria. This shows that AMPK is implicated in the immediate fragmentation of mitochondria seen in mitochondria seen in exercise, as its absence diminished this observation. The mechanism and rationale behind the increased fusion 12 hours after exercise is worth delving into, along with conducting the same assay with a recovery of 24 hours. As already mentioned, the sample size for this data is small and needs to be supported with more replications.

In *mdt-15* mutants, there is a remarkable rise in the Class 2 muscle cells. This implies an increased fusion of the mitochondria due to exercise-induced energy demands, which is starkly differing to the wild-type muscle cells that show mitochondrial fragmentation due to exercise. The mechanisms behind these observations may involve an enhanced fusion process to meet the cellular energy demands, one that the mdt-15 mutant is unable to do with fragmented mitochondria. Again, this data needs to be authenticated through replication.

It was determined that wild-type animals at the L4 stage show a fragmentation of mitochondria, an increase in intermitochondrial distance (IMD), and a reduction in mitochondrial density right after a 90-minute swim exercise session. The fragmentation of mitochondria is likely be due to the activation of AMPK signalling. AMPK is also known to physically interact with MFF, which participates in the process of fission (40, 41). The increase in IMD is either indicative of the

translocation of mitochondria to serve the local energy demands within the neuron, or mitophagy as a form of quality control. It is worth investigating what processes are responsible for this observation, and components that can settle this question are MIRO and TRAK for transport of mitochondria, and PINK/Parkin for mitophagy. Finally, the reduction in mitochondrial density can be attributable to mitophagy or even intercellular transfer of mitochondria to meet energy demands of other tissues (53).

The mitochondrial density of the L4 worms remains constant throughout their development into A1 adults, as already reported by Mondal et al. (2021) (51), giving further credence to the observed data. The increase in mitochondrial load and average area in mid-L4 stage are unexpected observations that need to be further validated. Swim exercise seems to intermittently add to this rise seen developmentally; however, why the effects of the exercise remain transitory needs to be probed further. Aspect ratio also shows an increase 24 hours after exercise, which may indicate to a promotion of mitochondrial fusion resulting in more elongated mitochondria.

Contrastingly, there were no such morphological alterations by exercise seen in the neuronal mitochondria of A3 worms. This implies that either the swim exercise assay is not enough to induce mitochondrial morphology alterations, or that using morphology as an indicator of the function of the mitochondria has limited utility. The functional integrity of the mitochondrial units is worth exploring, to ensure that the swim assay is indeed causing a shift in the energy demands of the PLM neuron and in the function of mitochondria.

In axotomized A3 worms, no major changes were observed in any morphology parameters in exercised or non-exercised conditions. This is likely due to the low sample size of the data presented. As discussed already, there is a significant drop in the pooled aspect ratio of worms subjected to exercise. The mitochondrial density is also verging on being significant. Thus, adding more samples to this incomplete dataset is likely to confer more conclusive results on the effects of exercise in axotomized worms on their neuronal morphology.

The motivation to uncover the link between mitochondrial dynamics and exercise-enhanced functional restoration of axotomized worms remains elusive. However, the involvement of AMPK signalling in changing the mitochondrial dynamics is clearly

observed in the muscle cells of *aak-2* and *mdt-15* mutants, both of which show different response to swim exercise. The fragmentation, increased motility and decreased density caused in neuronal mitochondria right after exercise in L4 worms is also indicative that exercise changes mitochondrial parameters. The rationale behind A3 worms not showing similar alterations needs to be explored further. Lastly, the decrease in pooled aspect ratio of axotomized and exercised worms as compared to unexercised ones is also suggestive of increased mitochondrial motility to meet the energy requirements posed by injury in the neuron, which needs to be further elucidated.

Chapter 6: Limitations and Future Directions

There are several limitations to this work. Observing morphology as an indicator of the mitochondria's function is can only partially answer how mitochondria are involved in regeneration, exercise, and the AMPK signalling pathway. A better assessment of the membrane integrity of mitochondria will give a biochemical basis for determining the functional changes in the organelle. This can be the next step towards bolstering the data already presented.

The imaging of mitochondria in muscles and neurons can be done with Mitotracker Red CMXRos and TMRE (tetramethylrhodamine ethyl ester) staining to determine the membrane integrity of the organelle (55). Both these dyes are sequestered by healthy mitochondria with sturdy membranes. mtKeima or mtRosella can be used to determine the effects of mitophagy in the dynamics seen, to separate mitochondrial fragmentation caused by mitophagy with the same caused by fission (56). Staining animals with these and exercising them will further determine whether the fragmentation of mitochondria results in smaller stressed organelles. It will also resolve the limitations of observing the morphology in A3 worms, which don't show any alterations caused by exercise.

Moreover, determining the morphology at timepoints with smaller recovery periods (like 3 hours and 6 hours) can shed light on the temporal changes in the mitochondrial morphology by exercise. The same can be done for axotomized worms. Worms at older life stages (like A6) can also be done to examine the age-related variations in mitochondrial dynamics and their sensitivity in responding to swim exercise.

Finally, to better understand the role of AMPK signalling in exercise, *aak-2* and *mdt-15* mutants can be subjected to exercise with a recovery time of 3, 6, 12 and 24 hours to better fathom the temporal control of mitochondrial dynamics these components are involved in. The evaluation of neuronal mitochondria in *aak-2* and *mdt-15* mutants similarly can be done to understand the same in a tissue-specific manner.

References

1. Gray MW. Mitochondrial evolution. Cold Spring Harb Perspect Biol. 2012 Sep 1;4(9):a011403. doi: 10.1101/cshperspect.a011403. PMID: 22952398; PMCID: PMC3428767.
2. Campbell D, Zuryn S. The mechanisms and roles of mitochondrial dynamics in C. elegans. Semin Cell Dev Biol. 2024 Mar 15;156:266-275. doi: 10.1016/j.semcdb.2023.10.006. Epub 2023 Oct 31. PMID: 37919144.
3. Rangaraju, V., Calloway, N., and Ryan, T.A. (2014) Activity-Driven Local ATP Synthesis Is Required for Synaptic Function. *Cell* **156**, 825–835, https://doi.org/10.1016/j.cell.2013.12.042
4. Macaskill, A.F., Rinholm, J.E., Twelvetrees, A.E., Arancibia-Carcamo, I.L., Muir, J., Fransson, A. et al. (2009) Miro1 is a calcium sensor for glutamate receptor-dependent localization of mitochondria at synapses. *Neuron* **61**, 541–555, https://doi.org/10.1016/j.neuron.2009.01.030
5. Li, Z., Okamoto, K.-I., Hayashi, Y. and Sheng, M. (2004) The Importance of Dendritic Mitochondria in the Morphogenesis and Plasticity of Spines and Synapses. *Cell* **119**, 873–887, https://doi.org/10.1016/j.cell.2004.11.003
6. Chang, D. T.W., Honick, A.S. and Reynolds, I.J. (2006) Mitochondrial Trafficking to Synapses in Cultured Primary Cortical Neurons. *J. Neurosci.* **26**, 7035–7045, https://doi.org/10.1523/JNEUROSCI.1012-06.2006
7. Su¨ dhof, T.C. (2012) Calcium Control of Neurotransmitter Release. *Cold Spring Harb. Perspect. Biol.* **4**, a011353, https://doi.org/10.1101/cshperspect.a011353
8. Billups, B. and Forsythe, I.D. (2002) Presynaptic mitochondrial calcium sequestration influences transmission at mammalian central synapses. J. Neurosci. 22, 5840–5847, https://doi.org/10.1523/JNEUROSCI.22-14-05840.2002
9. Kowaltowski, A.J., Menezes-Filho, S.L., Assali, E.A., Gonc¸ alves, I.G., Cabral-Costa, J.V., Abreu, P. et al. (2019) Mitochondrial morphology regulates organellar Ca2+ uptake and changes cellular Ca2+ homeostasis. FASEB J. 33, 13176–13188, https://doi.org/10.1096/fj.201901136R
10. Divakaruni, S.S., Van Dyke, A.M., Chandra, R., LeGates, T.A., Contreras, M., Dharmasri, P.A. et al. (2018) Long-Term Potentiation Requires a Rapid Burst

of Dendritic Mitochondrial Fission during Induction. Neuron 100, 860–875, https://doi.org/10.1016/j.neuron.2018.09.025

11. Y. Wang, J. Nie, G. Ferrari, J. P. Rey-Lopez, L. F. M. Rezende, Association of physical activity intensity with mortality: A national cohort study of 403681 US adults. *JAMA Intern. Med.* 181, 203–211 (2021)
12. J. A. Hawley, M. Hargreaves, M. J. Joyner, J. R. Zierath, Integrative biology of exercise. Cell 159, 738–749 (2014).
13. Time course of myogenic and metabolic gene expression in response to acute exercise in human skeletal muscle, https://doi.org/10.1152/japplphysiol.01185.2004
14. Adult Hippocampal Neurogenesis: Regulation and Possible Functional and Clinical Correlates https://doi.org/10.3389/fnana.2018.00044
15. Journal of Neuroscience 7 May 2014, 34 (19) 6624 6633; https://doi.org/10.1523/JNEUROSCI.4972-13.2014
16. Koo JH, Cho IH. Effects of Treadmill Exercise on Mitochondrial Dynamic Function and Neuronal CellSurvival in Transgenic Mice Model of Alzheimer's Disease. Exerc Sci. 2016;25(1):18-26.
17. Smith, G.M., and Gallo, G. (2018). The role of mitochondria in axon development and regeneration. Dev. Neurobiol. 78, 221–237.
18. Richardson CE, Shen K (2019) Neurite development and repair in worms and flies. Annu Rev Neurosci 42:209–226.
19. Ghosh-Roy A, Wu Z, Goncharov A, Jin Y, Chisholm AD. Calcium and cyclic AMP promote axonal regeneration in Caenorhabditis elegans and require DLK-1 kinase. J Neurosci. 2010 Mar 3;30(9):3175-83. doi: 10.1523/JNEUROSCI.5464-09.2010. PMID: 20203177; PMCID: PMC2921707.
20. Chen L, Chuang M, Koorman T, Boxem M, Jin Y, Chisholm AD. 2015. Axon injury triggers EFA-6 mediated destabilization of axonal microtubules via TACC and doublecortin like kinase. eLife 4:e08695
21. Han SM, Baig HS, Hammarlund M. Mitochondria Localize to Injured Axons to Support Regeneration. Neuron. 2016 Dec 21;92(6):1308-1323. doi: 10.1016/j.neuron.2016.11.025. PMID: 28009276; PMCID: PMC5364819.
22. Cartoni, R., Norsworthy, M. W., Bei, F., Wang, C., Li, S., Zhang, Y., … He, Z. (2016). The Mammalian-Specific Protein Armcx1 Regulates Mitochondrial

Transport during Axon Regeneration. Neuron, 92(6), 1294–1307. https://doi.org/10.1016/j.neuron.2016.10.060

23. Richardson CE, Shen K. Neurite Development and Repair in Worms and Flies. Annu Rev Neurosci. 2019 Jul 8;42:209-226. doi: 10.1146/annurev-neuro-070918-050208. Epub 2019 Mar 18. PMID: 30883262.
24. E. Machiela, et al., Disruption of mitochondrial dynamics increases stress resistance through activation of multiple stress response pathways, FASEB J. 34 (6) (2020) 8475–8492.
25. van der Bliek AM, Shen Q, Kawajiri S. Mechanisms of mitochondrial fission and fusion. Cold Spring Harb Perspect Biol. 2013 Jun 1;5(6):a011072. doi: 10.1101/cshperspect.a011072. PMID: 23732471; PMCID: PMC3660830.
26. Onraet, T., & Zuryn, S. (2024). C. elegans as a model to study mitochondrial biology and disease. *Seminars in Cell & Developmental Biology*, *154*(Pt A), 48–58. https://doi.org/10.1016/j.semcdb.2023.04.006
27. Campbell D, Zuryn S. The mechanisms and roles of mitochondrial dynamics in C. elegans. Semin Cell Dev Biol. 2024 Mar 15;156:266-275. doi: 10.1016/j.semcdb.2023.10.006. Epub 2023 Oct 31. PMID: 37919144.
28. Labrousse AM, Zappaterra MD, Rube DA, van der Bliek AM. C. elegans dynamin-related protein DRP-1 controls severing of the mitochondrial outer membrane. Mol Cell. 1999 Nov;4(5):815-26. doi: 10.1016/s1097-2765(00)80391-3. PMID: 10619028.
29. Cribbs JT, Strack S. Reversible phosphorylation of Drp1 by cyclic AMP-dependent protein kinase and calcineurin regulates mitochondrial fission and cell death. EMBO Rep. 2007 Oct;8(10):939-44. doi: 10.1038/sj.embor.7401062. Epub 2007 Aug 24. PMID: 17721437; PMCID: PMC2002551.
30. Park, J., Lee, D. G., Kim, B., Park, S.-J., Kim, J.-H., Lee, S.-R., … Lee, D.-S. (2015). Iron overload triggers mitochondrial fragmentation via calcineurin-sensitive signals in HT-22 hippocampal neuron cells. Toxicology, 337, 39–46. https://doi.org/10.1016/j.tox.2015.08.009
31. J.C. Campos, et al., Exercise preserves physical fitness during aging through AMPK and mitochondrial dynamics, Proc. Natl. Acad. Sci. 120 (2) (2023), e2204750120.

32. S.N. Chaudhari, E.T. Kipreos, Increased mitochondrial fusion allows the survival of older animals in diverse C. elegans longevity pathways, Nat. Commun. 8 (1) (2017), 182.
33. Michaelis, J.B., Brunstein, M.E., Bozkurt, S. *et al.* Protein import motor complex reacts to mitochondrial misfolding by reducing protein import and activating mitophagy. *Nat Commun* **13**, 5164 (2022). https://doi.org/10.1038/s41467-022-32564-x
34. Taubert S, Van Gilst MR, Hansen M, Yamamoto KR. A Mediator subunit, MDT-15, integrates regulation of fatty acid metabolism by NHR-49-dependent and -independent pathways in C. elegans. Genes Dev. 2006 May 1;20(9):1137-49. doi: 10.1101/gad.1395406. PMID: 16651656; PMCID: PMC1472473.
35. Kasai S, Shimizu S, Tatara Y, Mimura J, Itoh K. Regulation of Nrf2 by Mitochondrial Reactive Oxygen Species in Physiology and Pathology. Biomolecules. 2020 Feb 17;10(2):320. doi: 10.3390/biom10020320. PMID: 32079324; PMCID: PMC7072240.
36. Beale EG. 5'-AMP-activated protein kinase signaling in Caenorhabditis elegans. Exp Biol Med (Maywood). 2008 Jan;233(1):12-20. doi: 10.3181/0705-MR-117. PMID: 18156301.
37. Steinberg, G.R., Hardie, D.G. New insights into activation and function of the AMPK. *Nat Rev Mol Cell Biol* **24**, 255–272 (2023). https://doi.org/10.1038/s41580-022-00547-x
38. Nelson ME, Parker BL, Burchfield JG, Hoffman NJ, Needham EJ, Cooke KC, Naim T, Sylow L, Ling NX, Francis D, Norris DM, Chaudhuri R, Oakhill JS, Richter EA, Lynch GS, Stöckli J, James DE. Phosphoproteomics reveals conserved exercise-stimulated signaling and AMPK regulation of store-operated calcium entry. EMBO J. 2019 Dec 16;38(24):e102578. doi: 10.15252/embj.2019102578. Epub 2019 Aug 5. Erratum in: EMBO J. 2020 Apr 15;39(8):e104246. doi: 10.15252/embj.2019104246. PMID: 31381180; PMCID: PMC6912027.
39. Chen Z, Lei C, Wang C, Li N, Srivastava M, Tang M, Zhang H, Choi JM, Jung SY, Qin J, Chen J. Global phosphoproteomic analysis reveals ARMC10 as an AMPK substrate that regulates mitochondrial dynamics. Nat Commun.

2019 Jan 10;10(1):104. doi: 10.1038/s41467-018-08004-0. PMID: 30631047; PMCID: PMC6328551.

40. Losón OC, Song Z, Chen H, Chan DC. Fis1, Mff, MiD49, and MiD51 mediate Drp1 recruitment in mitochondrial fission. Mol Biol Cell. 2013 Mar;24(5):659-67. doi: 10.1091/mbc.E12-10-0721. Epub 2013 Jan 2. PMID: 23283981; PMCID: PMC3583668.
41. Hung CM, Lombardo PS, Malik N, Brun SN, Hellberg K, Van Nostrand JL, Garcia D, Baumgart J, Diffenderfer K, Asara JM, Shaw RJ. AMPK/ULK1-mediated phosphorylation of Parkin ACT domain mediates an early step in mitophagy. Sci Adv. 2021 Apr 7;7(15):eabg4544. doi: 10.1126/sciadv.abg4544. PMID: 33827825; PMCID: PMC8026119.
42. Drake JC, Wilson RJ, Laker RC, Guan Y, Spaulding HR, Nichenko AS, Shen W, Shang H, Dorn MV, Huang K, Zhang M, Bandara AB, Brisendine MH, Kashatus JA, Sharma PR, Young A, Gautam J, Cao R, Wallrabe H, Chang PA, Wong M, Desjardins EM, Hawley SA, Christ GJ, Kashatus DF, Miller CL, Wolf MJ, Periasamy A, Steinberg GR, Hardie DG, Yan Z. Mitochondria-localized AMPK responds to local energetics and contributes to exercise and energetic stress-induced mitophagy. Proc Natl Acad Sci U S A. 2021 Sep 14;118(37):e2025932118. doi: 10.1073/pnas.2025932118. PMID: 34493662; PMCID: PMC8449344.
43. Ghosh-Roy A, Chisholm AD. Caenorhabditis elegans: a new model organism for studies of axon regeneration. Dev Dyn. 2010 May;239(5):1460-4. doi: 10.1002/dvdy.22253. PMID: 20186917; PMCID: PMC3069807.
44. Hammarlund M, Jin Y. Axon regeneration in C. elegans. Curr Opin Neurobiol. 2014 Aug;27:199-207. doi: 10.1016/j.conb.2014.04.001. Epub 2014 May 4. PMID: 24794753; PMCID: PMC4122601.
45. Laranjeiro, R., Harinath, G., Burke, D. *et al.* Single swim sessions in *C. elegans* induce key features of mammalian exercise. *BMC Biol* **15**, 30 (2017). https://doi.org/10.1186/s12915-017-0368-4
46. Kumar S, Behera S, Basu A, Dey S, Ghosh-Roy A. Swimming Exercise Promotes Post-injury Axon Regeneration and Functional Restoration through AMPK. eNeuro. 2021 Jun 16;8(3):ENEURO.0414-20.2021. doi: 10.1523/ENEURO.0414-20.2021. PMID: 34031101; PMCID: PMC8211466.

47. Beckers A, Masin L, Van Dyck A, Bergmans S, Vanhunsel S, Zhang A, Verreet T, Poulain FE, Farrow K, Moons L. Optic nerve injury-induced regeneration in the adult zebrafish is accompanied by spatiotemporal changes in mitochondrial dynamics. Neural Regen Res. 2023 Jan;18(1):219-225. doi: 10.4103/1673-5374.344837. PMID: 35799546; PMCID: PMC9241429.
48. Cheng XT, Huang N, Sheng ZH. Programming axonal mitochondrial maintenance and bioenergetics in neurodegeneration and regeneration. Neuron. 2022 Jun 15;110(12):1899-1923. doi: 10.1016/j.neuron.2022.03.015. Epub 2022 Apr 16. PMID: 35429433; PMCID: PMC9233091.
49. Basu A, Dey S, Puri D, Das Saha N, Sabharwal V, Thyagarajan P, Srivastava P, Koushika SP, Ghosh-Roy A (2017) let-7 miRNA controls CED-7 homotypic adhesion and EFF-1-mediated axonal selffusion to restore touch sensation following injury. Proc Natl Acad Sci USA 114:E10206–E10215.
50. Laranjeiro R, Harinath G, Hewitt JE, Hartman JH, Royal MA, Meyer JN, Vanapalli SA, Driscoll M. Swim exercise in *Caenorhabditis elegans* extends neuromuscular and gut healthspan, enhances learning ability, and protects against neurodegeneration. Proc Natl Acad Sci U S A. 2019 Nov 19;116(47):23829-23839. doi: 10.1073/pnas.1909210116. Epub 2019 Nov 4. PMID: 31685639; PMCID: PMC6876156.
51. Mondal S, Dubey J, Awasthi A, Sure GR, Vasudevan A, Koushika SP. Tracking Mitochondrial Density and Positioning along a Growing Neuronal Process in Individual *C. elegans* Neuron Using a Long-Term Growth and Imaging Microfluidic Device. eNeuro. 2021 Jul 6;8(4):ENEURO.0360-20.2021. doi: 10.1523/ENEURO.0360-20.2021. PMID: 34035072; PMCID: PMC8260276.
52. Morsci NS, Hall DH, Driscoll M, Sheng ZH. Age-Related Phasic Patterns of Mitochondrial Maintenance in Adult Caenorhabditis elegans Neurons. J Neurosci. 2016 Jan 27;36(4):1373-85. doi: 10.1523/JNEUROSCI.2799-15.2016. PMID: 26818523; PMCID: PMC4728731.
53. Vignais ML, Caicedo A, Brondello JM, Jorgensen C. Cell Connections by Tunneling Nanotubes: Effects of Mitochondrial Trafficking on Target Cell Metabolism, Homeostasis, and Response to Therapy. Stem Cells Int. 2017;2017:6917941. doi: 10.1155/2017/6917941. Epub 2017 Jun 4. PMID: 28659978; PMCID: PMC5474251.

54. Sheng ZH. The Interplay of Axonal Energy Homeostasis and Mitochondrial Trafficking and Anchoring. Trends Cell Biol. 2017 Jun;27(6):403-416. doi: 10.1016/j.tcb.2017.01.005. Epub 2017 Feb 20. PMID: 28228333; PMCID: PMC5440189.
55. Sarasija S, Norman KR. Analysis of Mitochondrial Structure in the Body Wall Muscle of *Caenorhabditis elegans*. Bio Protoc. 2018 Apr 5;8(7):e2801. doi: 10.21769/BioProtoc.2801. PMID: 29707607; PMCID: PMC5914529.
56. Sun, N., Malide, D., Liu, J. *et al.* A fluorescence-based imaging method to measure *in vitro* and *in vivo* mitophagy using mt-Keima. *Nat Protoc* **12**, 1576–1587 (2017). https://doi.org/10.1038/nprot.2017.060